

# Special Issue: Integrating ZooMS and Zooarchaeology: Methodological Challenges and Interpretive Potentials

## Integrating Morphology and ZooMS-Identified Fauna Provides Insights Into Species Diversity and Neanderthal-Carnivores Interactions in Shared Landscapes: Evidence From Picken's Hole, Britain

FIONA HOLLORAN\*

*UCL Institute of Archaeology, 31-34 Gordon Square, London WC1H 0PY, UNITED KINGDOM; [fiona.holloran.19@ucl.ac.uk](mailto:fiona.holloran.19@ucl.ac.uk)*

DELPHINE FRÉMONDEAU

*UCL Institute of Archaeology, 31-34 Gordon Square, London WC1H 0PY, UNITED KINGDOM; [d.fremondeau@ucl.ac.uk](mailto:d.fremondeau@ucl.ac.uk)*

LINDA WILSON

*University of Bristol Spelaeological Society, Bristol, BS8 1TH UNITED KINGDOM; [lindawilson@coly.org.uk](mailto:lindawilson@coly.org.uk)*

LOUISE MARTIN

*UCL Institute of Archaeology, 31-34 Gordon Square, London WC1H 0PY, UNITED KINGDOM; [louise.martin@ucl.ac.uk](mailto:louise.martin@ucl.ac.uk)*

RHIANNON E. STEVENS

*UCL Institute of Archaeology, 31-34 Gordon Square, London WC1H 0PY, UNITED KINGDOM; [rhiannon.stevens@ucl.ac.uk](mailto:rhiannon.stevens@ucl.ac.uk)*

\*corresponding author: Fiona Holloran; [fiona.holloran.19@ucl.ac.uk](mailto:fiona.holloran.19@ucl.ac.uk)

*submitted: 10 June 2024; revised: 20 September 2024; accepted: 26 September 2024*

*Guest Editors: Geoff M. Smith (School of Anthropology and Conservation, University of Kent, and Department of Archaeology, University of Reading), Karen Ruebens (Department of Archaeology, University of Reading, and Chaire de Paléanthropologie, CIRB, Collège de France), Virginie Sinet-Mathiot (PACEA and Bordeaux Proteome-CBMN, Université de Bordeaux), and Frido Welker (Globe Institute, University of Copenhagen)*

*Handling Editor in Chief: Erella Hovers*

### ABSTRACT

Reconstructing the faunal paleoecology of landscapes occupied by Neanderthals and their competitors is essential for a better understanding of their ecological niche, decisions, and behaviors. Late Pleistocene faunal assemblages in Britain are highly fragmented with interpretations relying on the morphologically identifiable portion of the assemblage and the indeterminate bone fragments often dismissed. This paper applies two methodologies (taphonomic analysis and zooarchaeology by mass spectrometry [ZooMS]) to extract data from morphologically indeterminate bone fragments recovered from the late Middle Paleolithic contexts of Picken's Hole, Somerset, and integrates these new data with the extant zooarchaeological study of the morphologically identifiable faunal specimens. Two thousand, two hundred and five indeterminate bone fragments from Unit 3 were categorized to mammal body size classes and broad element type, and taphonomic observations were recorded (weathering, carnivore bone surface modification, etc.). Then 708 samples were selected for ZooMS. The ZooMS-identified faunal spectrum agrees with Scott's (2018) study of the morphologically identifiable portion (henceforth termed 'morph'), indicating an open cool steppe tundra environment. The faunal proportions differ greatly between identification methods, however, especially when dental remains are removed. Woolly rhinoceros, mammoth, and horse have the lowest ZooMS to Morph identification ratios (high ZooMS-NISP and low morph-NISP), while grey wolf/arctic fox and reindeer have the highest (low ZooMS-NISP and high morph-NISP). In addition, while the morphology-identified portion is dominated by dentition and foot bones, the ZooMS-identified portion includes more rib and long bone fragments. Weathering stages overall are low and do not appear to be a primary cause of fragmentation, while carnivore gnawing and evidence of digestion are observed across most species and fragment sizes,

with carnivore digestion responsible for most fragmentation. The exception is grey wolf/arctic fox that display no evidence of predation activity, suggesting that they and Neanderthals may have used the site intermittently alongside repeated use by large carnivores. This paper underscores the significance of extracting and integrating information from indeterminate bone fragments to contribute to the understanding of assemblage accumulators, site occupation, and carnivore activities at Picken's Hole, while ongoing bone surface modification studies aim to provide insight into Neanderthal behavior and interactions with carnivores operating in a shared landscape.

## INTRODUCTION

In contrast to late Middle Paleolithic assemblages in mainland Europe (Mellars 1996; Richter 2016; Ruebens 2014), Neanderthal presence in Britain during MIS 3 is represented by clusters of sites with numerically small but technologically related artifact assemblages (e.g., Wookey Hole, Creswell Crags), suggesting short occupation periods and diverse use of multiple locations across the landscape (Ashton and Scott 2016; Jacobi 2000; Roe 1981; White and Pettitt 2011; Wragg Sykes 2017, 2018). Picken's Hole (Compton Bishop, Somerset) is a small cave containing late Middle Paleolithic archaeology. It is among several late Middle Paleolithic cave sites of varying significance in the Mendip Hills and, in particular, along the Axe River Valley (ApSimon et al. 2018; Balch 1947; Harrison 1977; Jacobi 2000; Proctor et al. 1996; Tratman et al. 1971). Picken's Hole appears to be an under-represented type of task site used for the primary stages of lithic tool manufacture; however, the prevalence of carnivore activity and high levels of bone fragmentation complicate the interpretation of site formation and human presence (Scott 2018; Wragg Sykes 2018). Lithics recovered at Picken's Hole came from unit 3. The accumulation of the unit 3 faunal material likely resulted from spotted hyaena activity (Scott 2018). Spotted hyaena are known to scavenge carcasses butchered by humans (Egeland et al. 2008; Prendergast and Domínguez-Rodrigo 2008), therefore understanding the processes that led to high fragmentation of the faunal assemblage at a hyaena den site, including possible human modifications, would enhance understanding of interactions between carnivores and Neanderthals, and potentially further document Neanderthal presence in the landscape. The investigation of highly fragmented bone with Zooarchaeology by Mass Spectrometry (ZooMS, Buckley et al. 2009), also referred to as collagen peptide mass fingerprinting, is used to taxonomically identify bone specimens to sub-family, genus, or species level. The use of ZooMS vastly increases the number of identified specimens (Welker et al. 2015), providing a more holistic picture of the species that occupied the same habitat and landscapes as Neanderthals. ZooMS also facilitates the contextualization of taphonomic characteristics of morphologically unidentifiable bone fragments enabling patterns in carnivore/human processing and post-depositional processes to be explored (i.e., Martisius et al. 2020; Ruebens et al. 2023; Sinent-Mathiot et al. 2019, 2023; Smith et al. 2024).

Here ZooMS identification and taphonomic analysis of morphologically unidentifiable bone fragments from the 1960's excavations at Picken's Hole are integrated with

previous zooarchaeological data from the morphologically identifiable bone portion of this assemblage (Scott 2018). Through untargeted ZooMS screening, this study aims to add to the dataset on faunal structure at the site, including taphonomic patterning, and further understanding of the role of carnivores in site formation.

## BACKGROUND

### THE SITE AND NEANDERTHAL PRESENCE

Picken's Hole (Figure 1) was excavated between 1961–1967 by the University of Bristol Spelaeological Society (UBSS) (ApSimon et al. 2018; Tratman 1964). The faunal and archaeological findings from the cave show that while Neanderthals used the cave, its primary function was a hyaena den (Scott 2018; Wragg Sykes 2018).

In terms of its size, the cave is relatively small, with an entrance approximately 1.5m wide which opens onto a 6m wide platform. The cave extends ~5m into a weathered limestone cliff face, with rapid constriction towards its end. The excavated area (Figure 2) includes the cave entrance and sloping platform immediately outside the cave entrance (squares A - F), and three trenches between 20–32m down slope (squares G, J, and K) (ApSimon et al. 2018). The Pleistocene faunal material was recovered from Units 3, 4, and 5, with lithic artifacts found in Unit 3 (Scott, 2018; Tratman, 1964). The cave entrance during the accumulation of Unit 5 was likely a small wolf-sized opening, with a roof collapse during Unit 4 accumulation widening this entrance and later becoming a level-floored recessed shelter in the cliff-face during Unit 3 (P.L. Smart, personal communication). Finds recovered from Unit 3 include 37 lithic artifacts and over 3000 faunal specimens (Scott 2018; Wragg Sykes 2018). In places where Unit 3 appeared undisturbed, 500 find spots were three-dimensionally recorded (ApSimon and Smart 2018). The lithology of Unit 3 varies between clay loam, silty loam, and sandy loam, ranging in thickness from 80–50cm east to west (Figure 3) (ApSimon and Smart 2018). There are inconsistencies in the assignment of sub-contexts across the site, which complicates site formation interpretation, however, lithic refits show that vertical movement is minimal while horizontal movement is significant (Wragg Sykes 2018).

The small collection of stone tools at Picken's Hole has been thoroughly analyzed. It is evident that while there are technological commonalities with other late Middle Paleolithic sites in Britain, such as sites in Creswell Crags (Jacobi 2004) and those in the nearby Mendip region, there are some

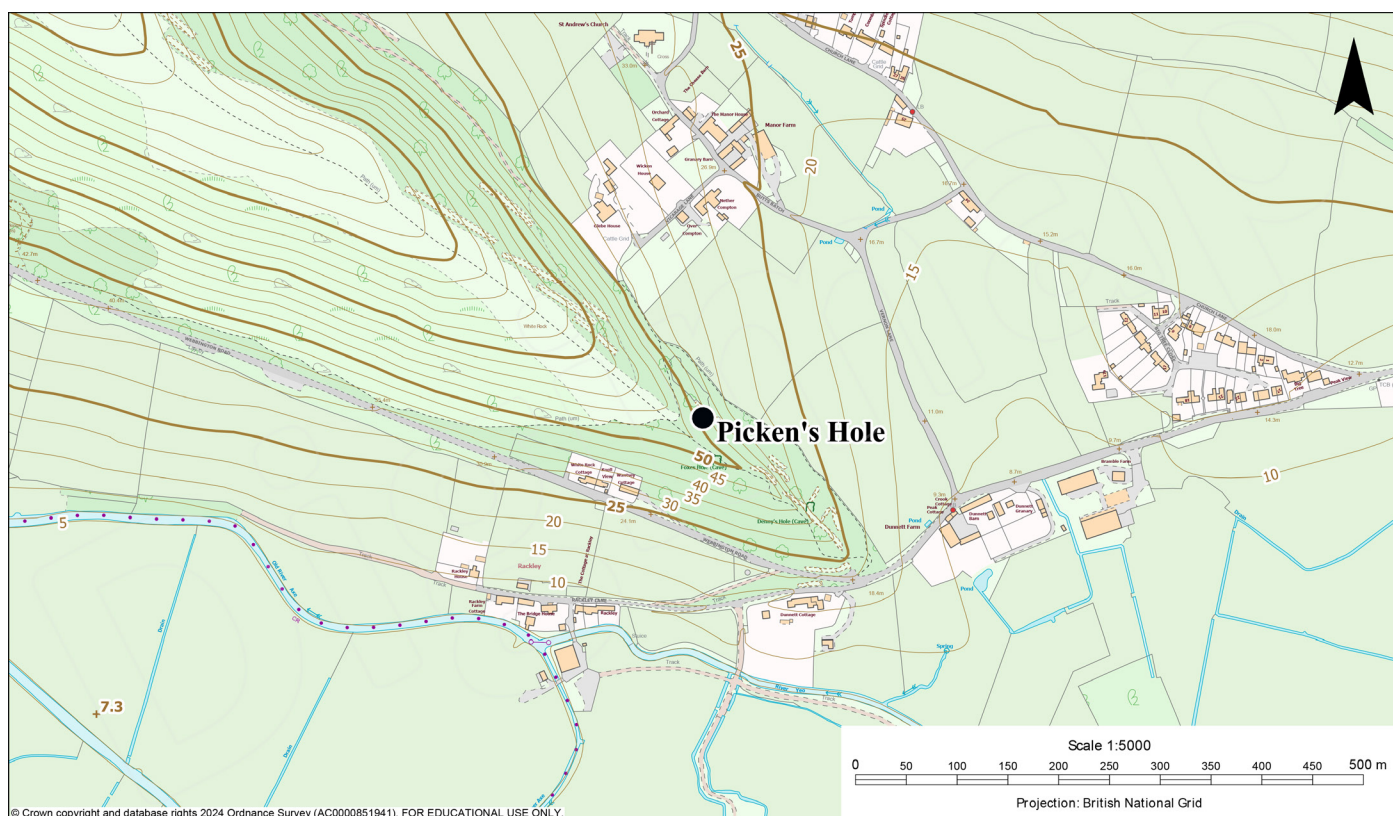


Figure 1. Picken's Hole on Crook Peak, overlooking Compton Bishop in Somerset (ST 3965 5502) (map created using Digimap Ordnance Survey Collection: <https://digimap.edina.ac.uk>) © Crown copyright and database rights 2024 Ordnance Survey [100025252]).

idiosyncrasies in the represented lithics that set Picken's Hole apart (Tratman 1964; Wragg Sykes 2018). The lithic artifacts include 29 flint or chert debitage, 5 chert cores, 1 chert hammerstone, 1 possible quartzite hammerstone, and 1 secondarily retouched chert piece (Wragg Sykes 2018). While chert is available regionally and near the cave, flint may have been sourced from further afield, such as a local riverbed (Bond 2004; Wragg Sykes 2018). Picken's Hole appears to have been used for primary stage reduction of flint and chert flakes from cores, and possibly maintaining bifaces that were then transported away (Wragg Sykes 2018). Similarities in the artifacts found at Uphill and Hyaena Den suggest that Picken's Hole was used in conjunction with other sites along the Mendip escarpment, overlooking the River Axe and the Somerset plain, perhaps over a long period of time and by different Neanderthal groups (Jacobi 2000; Jacobi et al. 2006; Wragg Sykes 2018).

### CHRONOLOGY AND ENVIRONMENT

There are 17 radiocarbon dates recorded from Picken's Hole. Six of these were analyzed before ultrafiltration (Higham et al. 2006) was introduced and are not considered further here (after Currant and Jacobi 2011), including three from Unit 3 and three from Unit 5 (Mullan 2018). The remaining 11 radiocarbon dates are on faunal specimens from Picken's Hole Unit 3 and suggest ages of >50–37 ka cal BP, consistent with MIS 3 (Figure 4; Supplementary Table S1) (Jacobi et al. 2009; Mullan 2018). Some radiocarbon

dates fall outside the calibration range (Reimer et al. 2020) and are considered older still. Therefore, the accumulation of Unit 3 may have spanned most of MIS 3, including several rapid and significant climatic shifts (Dansgaard et al. 1993; Rasmussen et al. 2014). The faunal spectrum found alongside the lithics, represented in Table 1 below, is attributable to the biostratigraphic zone defined as the Pin Hole mammal assemblage-zone (MAZ), which describes a common faunal assemblage type found throughout Britain during MIS 3, allowing for local variation (Currant and Jacobi 2011). Late Middle Paleolithic sites in the region with a similar faunal spectrum include Badger Hole (Balch 1947), Coygan Cave (Aldhouse-Green et al. 1995), Hyaena Den (Balch 1947; Jacobi et al. 2006; Tratman et al. 1971), Kents Cavern (Campbell and Sampson 1971; Pengelly 1884), Rhinoceros Hole (Proctor et al. 1996), Tornewton Cave (Sutcliffe and Zeuner 1962), Uphill Quarry Caves (Harrison 1977), and Windmill Cave (Pengelly 1873; Pettitt and White 2012). The Pin Hole MAZ is consistent with the vast and highly productive non-analogous ecosystem commonly referred to as the mammoth steppe that dominated from north-western Europe to Alaska during MIS 3. The mammoth steppe was a steppe-tundra mosaic landscape made up of cold and arid-adapted vegetation dominated by grasses that was highly resilient to climatic fluctuations and supported a high volume and diversity of large and very large herbivores (Guthrie 1982; Hibbert 1982; Kahlke 2014; Schwartz-Narbonne et al. 2019). Proxy records agree



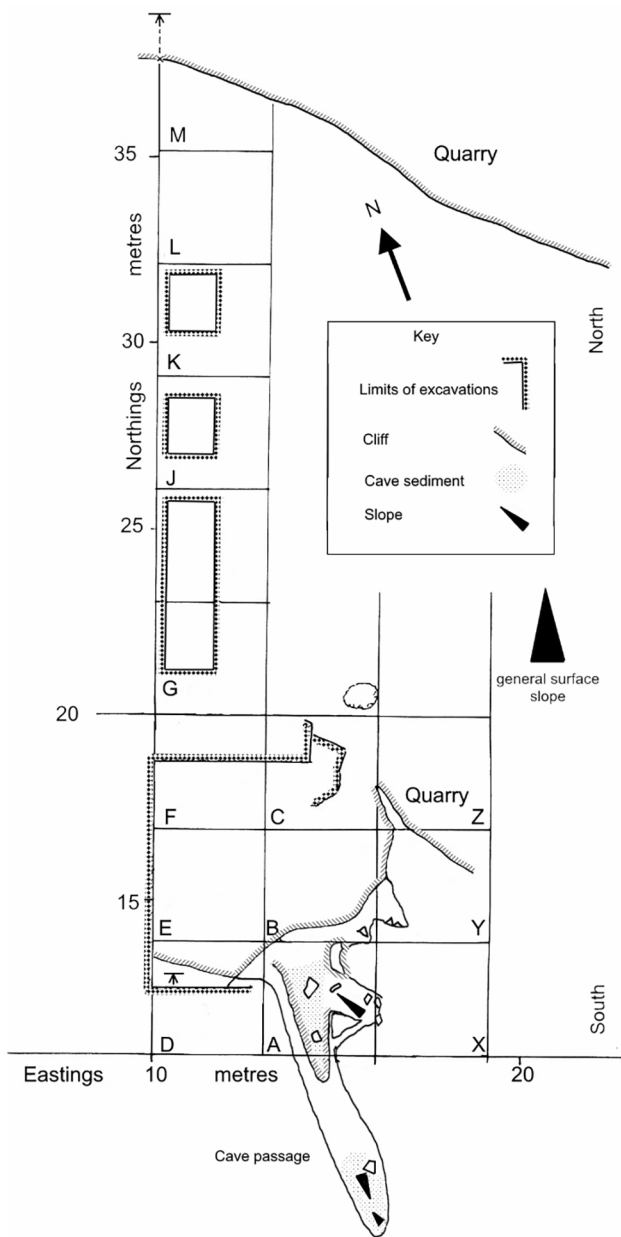


Figure 2. Site plan showing grid square and trench locations (map recreated from Figure 2 in ApSimon et al. 2018).

that southern Britain during MIS 3 was an open herbaceous grassland environment, with some marsh, sparse stands of small trees, and temperatures varying from cool, with summers like today and winters  $\sim 2^{\circ}\text{C}$  cooler, to harsher more continental conditions, with summers  $\sim 4^{\circ}\text{C}$  cooler than today and winters colder by  $\sim 15^{\circ}\text{C}$  (Langford et al. 2014; Lewis et al. 2006). Although mollusk and beetle records indicate such variation in conditions, with vast differences in expected temperature tolerances, there lacks an available discrete signal regarding vegetation reactions to rapid climatic changes (Langford et al. 2014). Mammoth (*Mammuthus primigenius*), horse (*Equus ferus*), and woolly rhinoceros (*Coelodonta antiquitatis*) may have been better suited to grass-dominated environments, making them likely to be more abundant in this landscape than species more reli-

ant on herbaceous vegetation, such as red deer (*Cervus elaphus*), bison (*Bison bonasus*), and reindeer (*Rangifer tarandus*) (Guthrie 1982; Scott 2018).

## METHODOLOGY

### SAMPLE SELECTION AND TAPHONOMY METHODS

Scott's analysis of the faunal collection included taxon identification for 988 specimens, body part representation, estimated Minimum Number of Individuals (MNI), age profiles, sex ratios of the cervids, the degree of fragmentation (including fracture type if discernible), and bone surface modifications (gnawing, burning, butchery, weathering, and acid etching) (Scott 1986, 2018). Specimens were all hand collected and although 500 finds are described as being three-dimensionally recorded (ApSimon and Smart 2018), no specific location records, other than context, were found with the specimens analyzed in this study.

The indeterminate faunal specimens from Unit 3 studied here are curated at the University of Bristol Spelaeological Society (UBSS). Many of the indeterminate specimens were stored in bags and boxes labelled 'Unit 3 Bone Scrap.' The storage location, date, or year of recovery, as available, and context were recorded for each specimen. Out of the 2380 specimens assessed, 130 were stones or other inorganic materials, which were removed from further analysis. There were also 40 tooth fragments that were removed because this study was targeting bone (the taphonomic signatures used here are only applicable to bone). The indeterminate bone fragments included 61 fragments with large modern breaks, and 67 fragments that bore relatively small modern breaks. Those with large modern breaks were removed from further analysis, to ensure that specimens were not assessed more than once, while those with small modern breaks were included, where the portion broken was unlikely to be a fragment large enough to accidentally re-sample. The remaining 2149 indeterminate bone fragments were all recorded, the smallest of which was 8mm in length. Each fragment was weighed in milligrams, the maximum dimension was measured using a ruler, and width and cortical thickness were taken for long bone fragments using a digital caliper. Each fragment was then analyzed and recorded according to the following attributes: mammal size class (Supplementary Table S2), bone element type (long bone, rib, vertebra, skull, indeterminate, etc.), weathering stage (0–5), abrasion (0–3), corrosion (<10%, 10–25%, 25–50%, 50–75%, 75–100%), root etching (0–2), break morphology (helical, longitudinal, stepped, diagonal, transverse), depositional bone surface modifications (polished, pitted, stained), carnivore modifications (gnawing, tooth notches, digestion, acid etched holes), and human modifications (cut marks, chopping marks, burning) (Andrews and Cook 1990; Behrensmeier 1978; Binford 1981; Bunn et al. 1986; Fernández-Jalvo and Andrews 2016; Fisher 1995; Marra 2013; Meloro et al. 2007; Villa and Mahieu 1991).

While Picken's Hole stands out as a Paleolithic site in Britain that has been excavated and documented in detail,



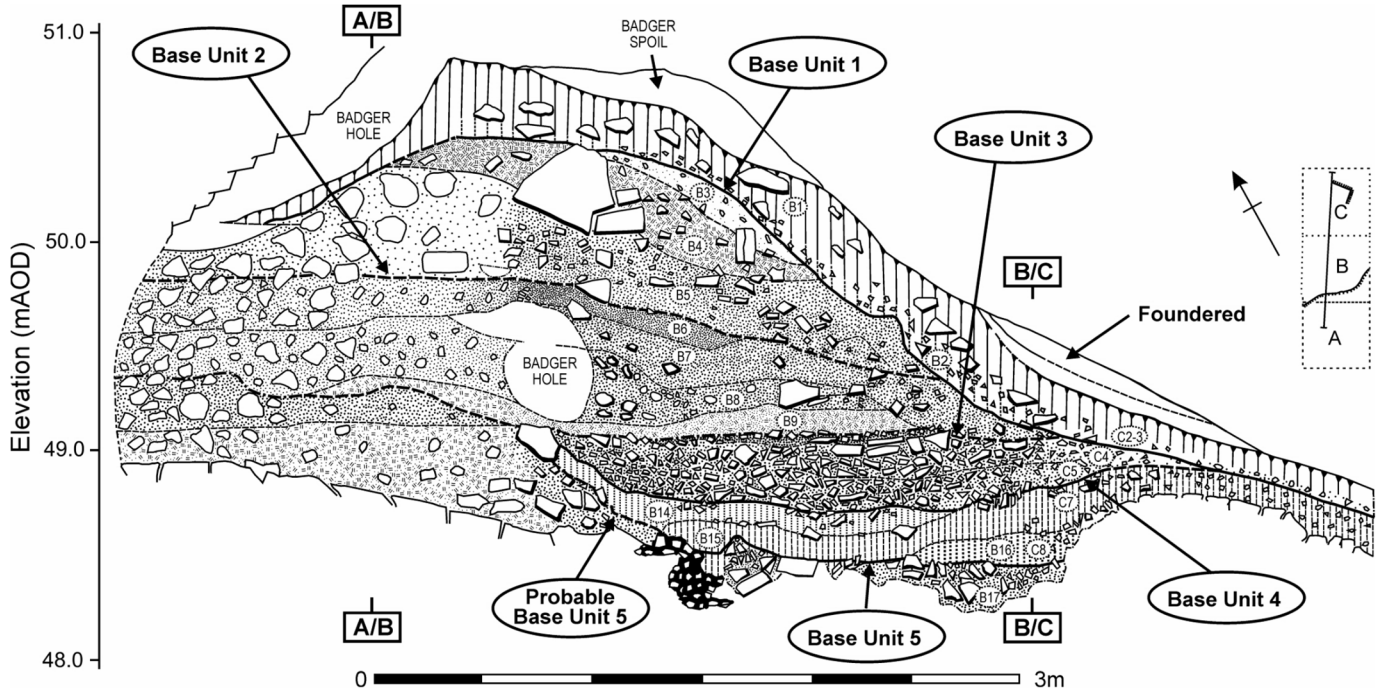


Figure 3. West facing section of the trial trench, which corresponds with squares A - C (ApSimon and Smart 2018). Contexts within these units were attributed by square and are not consistent between squares. This is due to lateral variation and the collapse of a key reference section part way through excavation (ApSimon and Smart 2018). Thus, contexts that could be cross correlated across the site are referred to more recently as 3B and 3D in the excavation publications and here correspond to contexts labelled B6 and B8. Since the recording of contexts within each unit was not consistent across the site, they are not relied on for this study (drawing recreated from Figure 8 in ApSimon et al. 2018).

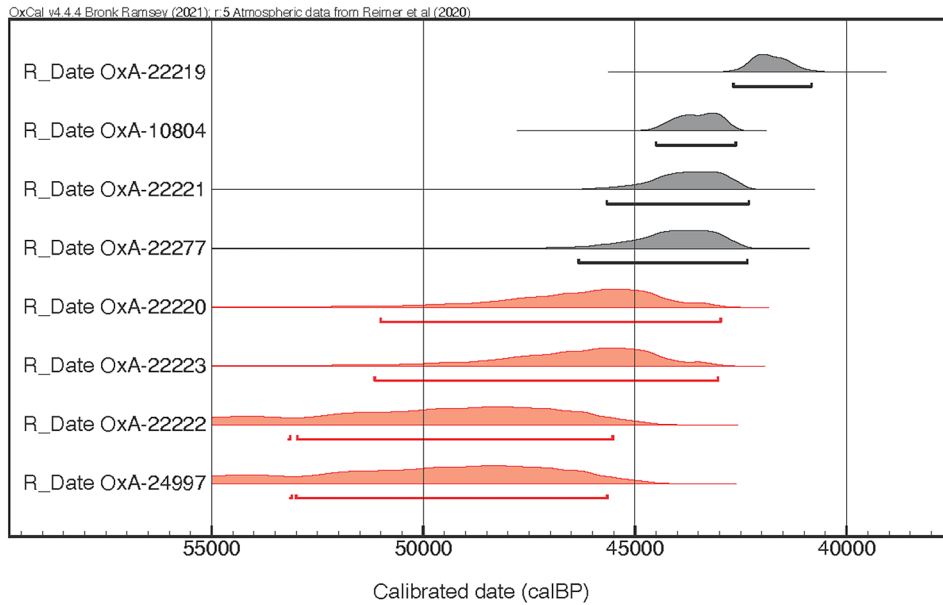


Figure 4. Ultra-filtered calibrated radiocarbon dates (cal BP) for faunal remains from Picken's Hole, Unit 3. Lab numbers and uncalibrated radiocarbon ages are reported in Mullen (2018). IntCal20 was used for calibration using OxCal online (<https://c14.arch.ox.ac.uk/oxcal/OxCal.html> 30/01/2024). Shown in red are four dates that may fall outside of the calibration range.

there are some inconsistencies in the recording of contexts. Layers 3B and 3D, within Unit 3 (which correspond to contexts labelled B6 and B8 in Figure 3) are the contexts from which the lithic artifacts were recovered. Ideally, the faunal material from these contexts would be targeted for this study, however, sub-contexts within the Units were attributed by square and are not consistent between squares. This is due to lateral variation in the sedimentary sequence and the collapse of a key reference section part way through excavation (Apsimon and Smart 2018). Therefore, although sub-contexts are considered, they are disregarded for the formal analysis of this study.

## ZOOMS METHOD

Of the 2149 indeterminate bone fragments recorded, 708 were selected for ZooMS analysis using the following criteria. The selected specimens included the 388 fragments that were identifiable to bone element type, excluding the 40 tooth fragments as noted above. The 1761 remaining indeterminate bone fragments were allocated to groups based on their maximum dimension (<2cm [n=409], 2–3cm [n=770], 3–4cm [n=375], 4–5cm [n=139], >5cm [n=68]) and 64 specimens were randomly selected from each group, totaling 320. ZooMS sample pre-treatment and analysis were conducted at the biomolecular archaeology laboratories within the UCL Institute of Archaeology (London, UK). The protocols followed are well established (Buckley et al. 2009; van Doorn et al. 2011; Wang et al. 2021). All fragments were processed using the ammonium-bicarbonate (AmBic) buffer protocol (van Doorn et al. 2011). Approximately 10–20mg bone chips were cut from the bone fragments using either a drill or clippers and placed into 96-well plates and covered with 100µl of 50mM AmBic overnight at ambient room temperature to clean and remove any soluble contamination. The 96-well plates were then centrifuged, and the supernatant discarded. Each sample was then covered again with 100µl of 50mM AmBic for one hour at 65°C to extract the soluble protein from the bone chips (van Doorn et al. 2011). The 96-well plates were then centrifuged and 50µl of the gelatinized sample was transferred to two new 96-well plates. One plate was retained and stored at -20°C for future use, while the other continued in pre-treatment. Trypsin solution (1µl of 0.4µl/µg) was then added to each sample and incubated for 16h at 37°C. The 96-well plate was centrifuged and 10µl of 0.5% Trifluoroacetic acid (TFA) was added to stop trypsin digestion. The peptides were then removed and purified using C18 ZipTips and eluted into a new 96-well plate with 50µl of 0.1% TFA in 50% Acetonitrile (ACN). To optimize the homogeneity of the crystals and improve the intensity and resolution of the resultant spectra, a pre-mixing method was used to spot samples. For each sample 5µl of purified peptides, 5µl 0.1% TFA in 50% ACN, and 10µl α-cyano-4-hydroxycinnamic acid (CHCA) solution (10mg/mL) were mixed (Wang et al. 2021) in a new 96-well plate and 1.5µl of the solution spotted immediately in triplicate onto the 48-spot MALDI plate. Spotted samples were then analyzed using a Shimadzu Matrix Assisted Laser Desorption Ionization Time

of Flight Mass Spectrometer (MALDI-8020 Mass Spectrometer) in linear mode, positive polarity, and with a blanking mass set at a  $m/z$  of 700. Calibration of the MALDI-ToF-MS was performed using Bruker Daltonics Peptide calibration Standard II (excluding Bradykinin Fragment 1-7). Spectra were obtained over a  $m/z$  range of 900–4000, using a low ( $m/z$  1200–1300) and/or medium ( $m/z$  1800), and high ( $m/z$  2500–3200) pulsed extraction mass to achieve the best resolution on both small and large peptides. Empty wells were processed alongside the samples, all of which returned empty spectra showing that no contamination was introduced during pre-treatment.

The spectra obtained from the MALDI were then processed in R using the MALDIquant and MALDIquantForeign packages (Gibb and Strimmer 2012). Smooth intensity was applied using the Savitzky-Golay method, and the baseline removed using the SNIP method. Spectra were then trimmed according to the pulsed extraction mass used (low:  $m/z$  1050–1700, medium:  $m/z$  1050–2200 or 1400–2200, high:  $m/z$  2100–3200), transformed and smoothed using the square root method and baseline removed once again (after Le Meillour et al. 2024). The resultant .msd files were then analyzed using mMass (Strohalm et al. 2010) with isotopic removal and signal to noise ratio of 1. This signal to noise ratio was chosen so as not to lose vital but low intensity determinate peptides, for example, those found at  $m/z$  1150–1250. The spectra were manually assessed for the presence of nine peptide markers and taxonomic identifications were made with reference to an existing database (Welker et al. 2016).

Due to the limitations of ZooMS identifications, some taxa were grouped, and others were assigned to species based on which species have been identified morphologically. Two sets of carnivores, spotted hyaena (*Crocuta crocuta*) and lion (*Panthera spelaea*), and grey wolf (*Canis lupus*) and arctic fox (*Vulpes lagopus*), could not be separated using ZooMS. For spotted hyaena and lion, this was due to insufficient peptide recovery at  $m/z$  2808/2820. Spotted hyaena and arctic fox remains are by far the most dominant in the morphologically identifiable portion, therefore, it is likely that most of the ZooMS-identified spotted hyaena/lion are also spotted hyaena, and that the wolf/arctic fox identifications are mostly arctic fox. However, lion and grey wolf are present in small quantities in the morphologically identifiable remains, and thus the possibility some of these indeterminate fragments being lion rather than hyaena and grey wolf rather than arctic fox cannot be discounted. The *Bos/Bison* classification includes a few potential species, however, only *Bison bison* (bison) was identified within the morphology-identified portion. The Cervid/*Saiga* classification also includes several possible species, however only *Cervus elaphus* (red deer) and *Megaloceros giganteus* (giant deer) were identified within the morphologically identifiable portion. It is clear that ZooMS identifications often include several possible species and cannot be narrowed down to one or another. While morphological identifications allow some specimens to be assigned to species, it seems cautionary to consider that ZooMS identifications/

classifications could potentially include all species that may have been within the geographical and temporal range of the site.

#### FRAGMENTATION ANALYSIS AND SKELETAL/BODY PART REPRESENTATION METHOD

Skeletal/body part representation and fragmentation analysis are key components in zooarchaeological analyses, which are useful for exploring carcass transport, accumulation processes, and subsistence strategies (Binford 1981; Klein and Cruz-Urbe 1984; Lyman 1994; Morin et al. 2017). The addition of ZooMS-identified specimens facilitates an examination of fragmentation and skeletal/body part representation at taxon level that may be impossible morphologically due to identifiability, and thus add greater detail to understanding faunal accumulations (Sinet-Mathiot et al. 2023). In this comparison there are biases in both identification methods that must be considered. Within the morphology-identified portion, certain taxa and skeletal elements are more easily identified. For example, *Bos/Bison*, horse, and red deer specimens can be difficult to distinguish once fragmented due to similarities in morphology, while the smaller size of reindeer means that if they are fractured to the same degree, the fragments are more likely to retain a greater proportion of the whole bone and some diagnostic features (Grayson 1984; Morin 2012; Pickering et al. 2006; Watson 1972, 1979). This results in a higher identification rate for reindeer. For the ZooMS-identified portion, the differential fragmentation rate between taxa and elements can inflate the Number of Identified Specimens (NISP). This is particularly problematic for rib and long bone shaft fragments, which means that ZooMS-NISP currently adds the most value in investigating patterns in species presence and carcass transport while the associated quantification in understanding relative faunal proportions must be applied with regard to the morphological component.

ZooMS to Morph identification ratios were calculated to investigate differences in faunal proportion between identification method. Teeth were removed from the morphological portion for this analysis because no teeth were identified using ZooMS and the purpose is to assess bone fragmentation. While it would be informative to include the 1441 unanalyzed bone fragments if they could be assigned to mammal size class, due to their indeterminate state, it was possible to assign only 10 to mammal size class 3 (medium-small) and 1 to mammal size class 9 (large). Therefore, they are not included in further analysis here. There are several approaches to investigating the level of fragmentation within zooarchaeology, such as using the ratio of the Minimum Number of Elements (MNE) to NISP per element (Lyman and Wolverton 2023; Wolverton 2002) or the ratio of Number of Recovered Specimens (NRSP) to NISP (Cannon 2013). Here the ratio of morphological NISP (morph-NISP) to ZooMS-NISP is examined. Thus, with the assumptions that ZooMS-NISP is dependent on morph-NISP, and skeletons of a similar size will produce a similar proportion of fragments, all things being equal, (Grayson 1984; Lyman 1994), it follows that taxa of the same mam-

mal size class should have similar ratios of morph-NISP to ZooMS-NISP. If their ratios are dissimilar, this will imply that the carcasses were treated differently or that the taphonomic histories of the bone specimens vary.

A comparison of skeletal/body part representation has been conducted for both morphology- and ZooMS-identified specimens. With the use of a comparative reference collection, Scott (1986, 2018) attempted to identify rib fragments and long bone diaphyses, on the understanding that hyaena were active at the site and likely destroyed many diagnostic attributes (Kruuk 1972). Therefore, the differences in body part representation between identification method are due to morphological identifiability rather than a decision to exclude commonly undiagnostic fragments. There may also be some bias introduced by the initial excavators prioritizing the collection of teeth over bone fragments (P.L. Smart, personal communication). To assess the differences between identification method, ZooMS-identified specimens were identified to element or element type where possible and grouped into categories (1: Antler/Horn/Tusk: antlers, horn, tusk; 2: Cranial: cranium, mandible, atlas, axis; 3: Thorax: ribs, remaining vertebrae, scapula, pelvis; 4: Limbs: humerus, radius, ulna, femur, tibia; 5: Feet: metacarpals, carpals, metatarsals, tarsals, phalanges; 6: ZooMS-identified long bone fragments; 7: Indeterminates: all fragments that could not be identified to element type). Since ZooMS-identified long bone fragments (LBF) could include long bone for the limbs or feet, LBF were reported separately from limb and foot bones. In addition, limb and foot bones were primarily identified morphologically while LBF were identified solely using ZooMS. Antlers, horns, and tusks were separated from cranial elements since they can inflate the result. Tusks were included with the antlers and horns, since, although they are dentition, they are present for only one species here (mammoth) and are more easily identified than tooth fragments. Dentition for the morphology-identified component were excluded when directly comparing morphology (n=283 [with teeth, n=988]) and ZooMS (n=679) identified species identification for select analyses (see below).

## RESULTS AND DISCUSSION

### FAUNAL PRESENCE AND PROPORTIONS

A total of 1667 bone specimens from Picken's Hole, Unit 3, were identified by either morphology or ZooMS. Faunal presence was assessed to see whether any taxa were added by ZooMS-identified fragments, and faunal proportions were calculated to establish to what degree ZooMS-NISP inflated total NISP. Changes in faunal presence may have implications for understanding the local ecology of the landscapes occupied by the Neanderthals, while differences in faunal proportions could indicate methodological bias in identifiability and be used to infer levels of fragmentation. Of the 708 bone fragments processed for ZooMS identification, 95.9% could be identified to species, genus, or family. The 10 ZooMS-identified taxa are, in order of prevalence, *Coelondonta antiquitatis* (woolly rhinoceros, 35.5%), *Rangifer*



*tarandus* (reindeer, 24.3%), *Equus* sp. (horse, 12.2%), *Crocota crocuta/Panthera* sp. (spotted hyaena/lion, 7.7%), *Cervus* sp./*Megaloceros* sp. (deer/giant deer, 6.8%), *Mammuthus primigenius* (mammoth, 6.2%), *Bos* sp./*Bison* sp. (bison, 5.6%), and between 2–5 fragments each of *Canis lupus/Vulpes lagopus* (grey wolf/arctic fox), *Vulpes vulpes* (red fox), and *Ursus* sp. (bear) (Table 1). These ZooMS identified presence and proportions are consistent through the sub-contexts 3B and 3D (Supplementary Table S3). For the 988 morphology-identified specimens, spotted hyaena is most prevalent (23.7%), followed by reindeer (18.6%), horse and woolly rhinoceros (16%), arctic fox (10%), bison (4.9%), red deer (4.8%), mammoth (3%), grey wolf (1.3%), and between 3–5 specimens of

giant deer, bear, and lion. No red fox was identified morphologically (see Table 1). Thus, faunal presence within the morphology- and ZooMS- identified portion agree, except for three small rib and long bone fragments of ZooMS-identified red fox.

Faunal proportions differ between identification methods. The largest differences are within the carnivores and some herbivores. Although 40 unidentified tooth fragments were not analyzed using ZooMS, it is unlikely that the addition of such a small sample size would significantly alter these proportions compared to the vast number of morphologically identified teeth. Arctic fox is much more highly represented morphologically (10%) than by ZooMS-iden-

**TABLE 1. MORPHOLOGICAL IDENTIFICATION RESULTS (Scott 2018) and ZooMS identification results (this study).\***

ZooMS ID Estimate (geographic)	ZooMS ID Estimate (after Morph)	Morphological ID	Morph		ZooMS		Morph + ZooMS	
			NISP	%NISP	NISP	%NISP	NISP	%NISP
<i>Canis lupus/Vulpes lagopus</i>	<i>Canis lupus/Vulpes lagopus</i>	<i>Vulpes lagopus</i>	70 (99)	24.7 (10)	2	0.3	83 (114)	8.6 (6.8)
		<i>Canis lupus</i>	11 (13)	3.9 (1.3)				
<i>Vulpes vulpes</i>					3	0.4	3 (3)	0.3 (0.2)
<i>Crocota crocuta/Panthera</i> sp.	<i>Crocota crocuta/Panthera leo</i>	<i>Crocota crocuta</i>	26 (234)	9.2 (23.7)	52	7.7	79 (289)	8.2 (17.3)
		<i>Panthera leo</i>	1 (3)	0.4 (0.3)				
<i>Rangifer tarandus</i>	<i>Rangifer tarandus</i>	<i>Rangifer tarandus</i>	125 (184)	44.2 (18.6)	165	24.3	290 (349)	30.1 (20.9)
<i>Ursus</i> sp.	<i>Ursus arctos</i>	<i>Ursus arctos</i>	0 (3)	0 (0.3)	5	0.7	5 (8)	0.5 (0.5)
<i>Cervus/Megaloceros/Saiga</i>	<i>Cervus elaphus/Megaloceros giganteus</i>	<i>Cervus elaphus</i>	12 (47)	4.2 (4.8)	46	6.8	62 (98)	6.4 (5.9)
		<i>Megaloceros giganteus</i>	4 (5)	1.4 (0.5)				
<i>Bos/Bison</i>	<i>Bison bison</i>	<i>Bison bison</i>	16 (48)	5.7 (4.9)	38	5.6	54 (86)	5.6 (5.2)
<i>Equus</i> sp.	<i>Equus ferus</i>	<i>Equus ferus</i>	4 (161)	1.4 (16.3)	83	12.2	87 (244)	9 (14.6)
<i>Mammuthus primigenius</i>	<i>Mammuthus primigenius</i>	<i>Mammuthus primigenius</i>	3 (30)	1.1 (3)	42	6.2	45 (72)	4.7 (4.3)
<i>Coelodonta antiquitatis</i>	<i>Coelodonta antiquitatis</i>	<i>Coelodonta antiquitatis</i>	11 (161)	3.9 (16.3)	241	35.5	252 (402)	26.2 (24.1)
<i>Bos/Bison/Rangifer tarandus</i>					2	0.3	2 (2)	0.2 (0.1)
<b>Total identified samples</b>			<b>283 (988)</b>	<b>100 (100)</b>	<b>679</b>	<b>95.9</b>	<b>962 (1667)</b>	<b>100 (100)</b>
Failed analyses (no collagen)					10	1.4		
Failed analyses (insufficient peptides)					19	2.7		
<b>Total failed analyses</b>					<b>29</b>	<b>4.1</b>		
<b>Total ZooMS analyzed bone</b>					<b>708</b>	<b>100</b>		
Total ZooMS unanalyzed indeterminate bone					1441			
Total ZooMS unanalyzed dental remains					40			

\*Number of Identified Specimens (NISP) and percentage NISP (%NISP) for each ID method used in this study. Species are reported in four sections according to mammal size class, from the top: 3: medium-small, 5: medium, 7: medium-large, 9: large. 'ZooMS ID Estimate (geographic)' is the identification of the morphologically unidentifiable portion of faunal specimens resulting from spectral analysis and species known to be present in Europe during MIS 3, 'ZooMS ID Estimate (after Morph)' is the species estimate based on the morphological identifications (data from this study) and 'Morphological ID' is the morphological identification from the anatomically identifiable portion of faunal specimens (data from Scott 2018) from Picken's Hole, Unit 3. Morph-NISP is presented: NISP without teeth (NISP with teeth). The failed analyses are reported according to whether the identification failed due to lack of collagen or insufficient (weak/absent) peptides. ZooMS-NISP excludes 1441 unanalysed indeterminate bone fragments and 40 unanalysed tooth fragments.

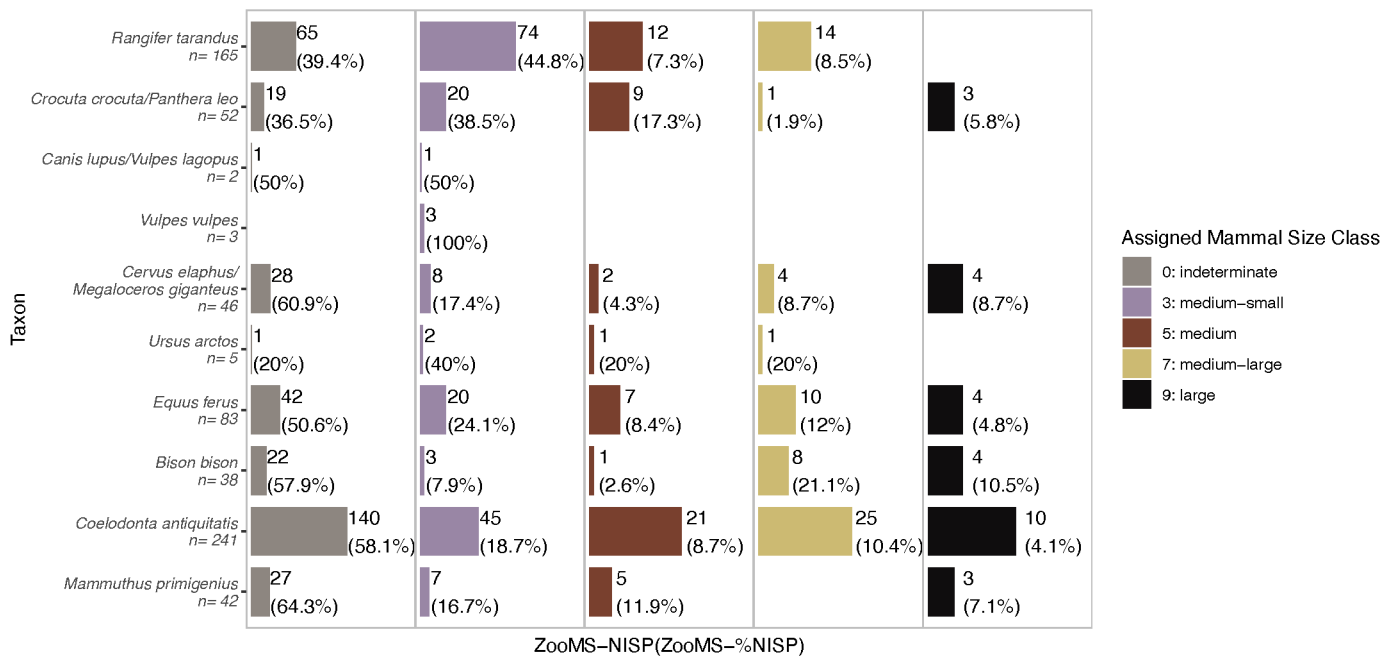


Figure 5. Comparison between the pre-analysis assigned mammal size class of ZooMS identified specimens and their species identity (medium-small: fox, hyaena, reindeer; medium: bear, red deer, giant deer; medium-large: bison, horse; large: mammoth, woolly rhinoceros; see methods).

tified fragments (wolf/arctic fox: 0.3%) and while spotted hyaena is the most highly represented species morphologically (23.7%), it is much less well represented in the ZooMS-identified portion (spotted hyaena/lion: 7.7%). For the herbivores, the greatest variability is with woolly rhinoceros (morph: 16%, ZooMS: 35.5%) and mammoth (morph: 3%, ZooMS: 6%) where in both cases the ZooMS-%NISP is twice or more the morph-%NISP (see Table 1). For all other herbivores, proportions are similar between identification method, with most ZooMS-%NISP marginally more than morph-%NISP, except for horse where ZooMS-%NISP is slightly less.

### Fragmentation Analysis: Identification Ratio

Disparities in faunal proportions between identification methods may potentially indicate variation in fragmentation patterns or identification rate between taxa. Teeth were removed from the morphological portion for this analysis (see Methods). Differences in identification rates for the morphological component can arise because some species, such as reindeer, are easier to distinguish when fragmented than bison and horse remains (Morin 2012). This is emphasized by the variability between mammal size class assignment and ZooMS species identification. Of the 679 ZooMS-identified samples, 334, primarily long bone and rib fragments, were assigned to mammal size class. The majority of the medium-small taxa are correctly assigned, for example 44.8% of reindeer remains were correctly assigned to 'medium-small', while none were assigned to the 'large' size class. While the 'medium-large' and 'large' sized taxa mostly unassigned or incorrectly assigned, for example, 58.1% of woolly rhinoceros fragments were un-

assigned, while 4.1% were assigned to the correct 'large' class (Figure 5). This demonstrates that mammal size class assignments are not accurate indicators of species identity as has been found elsewhere (Reubens et al. 2023; Sinet-Mathiot et al. 2019; 2023), and the low identifiability of fragmented 'large' size taxa within this assemblage. Therefore, taxa proportions are assessed by species identity mammal size class to reduce the impact of identification bias. The ratio of morph-NISP to ZooMS-NISP can inform on identification rates (Figure 6). The identification ratio is similar within the 'large' mammal size class, woolly rhinoceros (0.05) and mammoth (0.07). There is some variability within the 'medium-large' size class, where bison (0.4) has a higher ratio than horse (0.05), and horse matches ratios found within the 'large' size class. Taxa cannot be compared within the 'medium' size taxa as there are no bone specimens morphologically identified to bear; however, the deer/giant deer (0.3) identification ratio is similar to bison. There is much wider variability within 'medium-small' size class than the larger classes. Hyaena/lion (0.5) has a similar identification ratio to bison and deer/giant deer, while wolf/arctic fox (40.5) has the highest ratio of all taxa. Reindeer has the highest number of morphologically identifiable bone specimens of all taxa (which is possibly due to small fragments being identifiable) and has a higher identification ratio than hyaena/lion (0.8). Overall, the combined morphological and ZooMS identified specimens suggest that hyaena/lion, horse, reindeer, and woolly rhinoceros are the dominant taxa at this site, while woolly rhinoceros, mammoth, and horse have the lowest identification ratios, and wolf/arctic fox and reindeer the highest. Therefore, there appears to be variation in identifiability across the

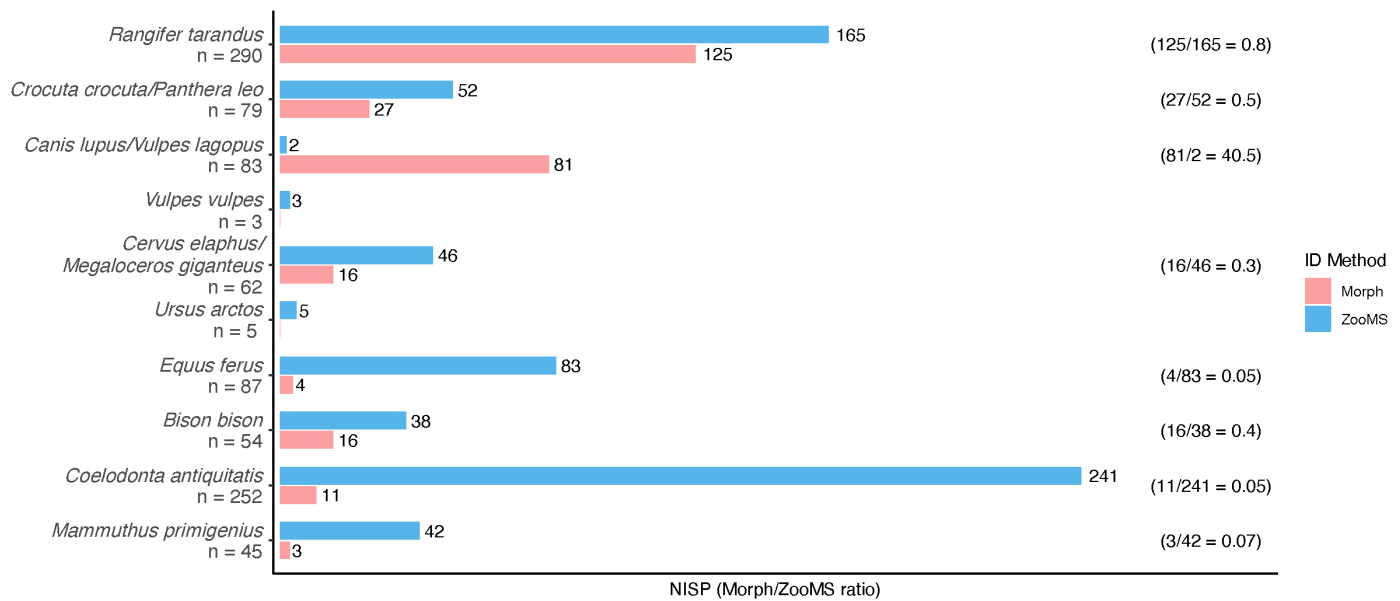


Figure 6. Number of morphologically identified specimens (morph-NISP)—excluding teeth ( $n=283$ ; data from Scott 2018)—versus number of ZooMS identified specimens (ZooMS-NISP) ( $n=677$ ; data from this study) for all taxa from Picken’s Hole, Unit 3. The axis labels are taxon/grouping,  $n$ =total NISP, excluding teeth. Data labels are taxon/grouping:  $n$ =morph-NISP, excluding teeth (ZooMS-NISP). Species groupings for morph-NISP to be relatable to the ZooMS-NISP include, in all cases, one dominant species (underlined): for the spotted hyaena/lion grouping, *Panthera leo* ( $n=3$ ) has been combined with *Crocuta crocuta* ( $n=234$ ); the grey wolf/arctic fox grouping combines *Canis lupus* (13) with *Vulpes lagopus* (99); and the deer/giant deer grouping includes *Megaloceros giganteus* (5) and *Cervus elaphus* (47).

‘medium-small’ and ‘medium-large’ taxa, despite similar body sizes. Identifiability can be examined in greater detail by assessing the length of ZooMS-identified fragments. While it would be worthwhile to consider the size distribution and taphonomic traits of the morphology-identified specimens as well (Discamps et al. 2024; Ruebens et al. 2023; Sinet-Mathiot et al. 2023), this is beyond the scope of the present study.

### ZooMS-Identified Specimens: Fragment Length

Fragment length was assessed for the ZooMS-identified portion to test whether difference in identifiability is linked to fragment length. Identifying patterns in the variation in the identifiability of fragments may aid interpretation of possible causes and intensity of fragmentation. Shapiro-Wilk normality tests showed that the maximum dimensions of all taxa are non-normally distributed, except bear ( $n=5$ ) which has a relatively small sample size (hyaena/lion:  $W=0.95$ ,  $p=0.03$ ; reindeer:  $W=0.91$ ,  $p<0.001$ ; deer/giant deer:  $W=0.92$ ,  $p=0.004$ ; bear:  $W=0.95$ ,  $p=0.7$ ; bison:  $W=0.80$ ,  $p<0.001$ ; horse:  $W=0.91$ ,  $p<0.001$ ; woolly rhinoceros:  $W=0.89$ ,  $p<0.001$ ; mammoth:  $W=0.93$ ,  $p=0.01$ ). ZooMS-identified fragment maximum dimension ranged from 1cm to 16.4cm, with a median of 3.5cm (IQR=2.2cm). The largest among these (8–16cm,  $n=26$ ) were anatomically unidentifiable due to lack of diagnostics and while 3 were also unidentifiable through ZooMS, the remaining 23 represent all seven of the most significant species: bison (5), deer/giant deer (5), woolly rhinoceros (4), horse (3), reindeer (3), hyaena/lion

(2), and mammoth (1). Overall, hyaena/lion (median=4 [IQR=2.2] cm) and deer/giant deer (4 [3] cm) have the longest fragments, followed by horse (3.8 [1.9] cm), bison (3.8 [2.5] cm), and mammoth (3.7 [2] cm), woolly rhinoceros (3.5 [2.1] cm), wolf/arctic fox (3.3 [0.1] cm), reindeer (3 [1.8] cm), bear (3 [1.1] cm), and red fox (2.1 [0.5] cm) (Supplementary Table S4). Reindeer has the largest proportion of <2cm fragments (28%) compared to >5cm (12%), while hyaena has the opposite pattern (13% <2cm and 27% >5cm) (Figure 7). Deer/giant deer has a mixed pattern, with both the largest proportion of <2cm (28%) and >5cm fragments (30%), this may be due to the amalgamation of two species of different mammal size class. Bison, horse, and mammoth have slight increases from smaller sized fragments (17–18%) to larger fragments (22–26%). Woolly rhinoceros is unique in that it has a relatively flat distribution, with similar proportions across the large and small sized fragments (18–19%) and a small increase (22%) for 2–4cm fragments.

The non-parametric Kolmogorov-Smirnov test (Gifford-Gonzalez 2018; Klein and Cruz-Urbe 1984) was chosen to compare fragment length frequencies of each taxon with  $n>30$ . The results show that there are no significant differences in the frequency of fragment length between species, regardless of mammal size class, except for reindeer. Reindeer fragments tend to be smaller than all other taxa (Figure 8; Supplementary Table S5), which agrees with the median that is also smaller than all taxa with  $n>30$  (see Supplementary Table S4). This suggests that reindeer fragments that are anatomically unidentifiable are smaller than those of



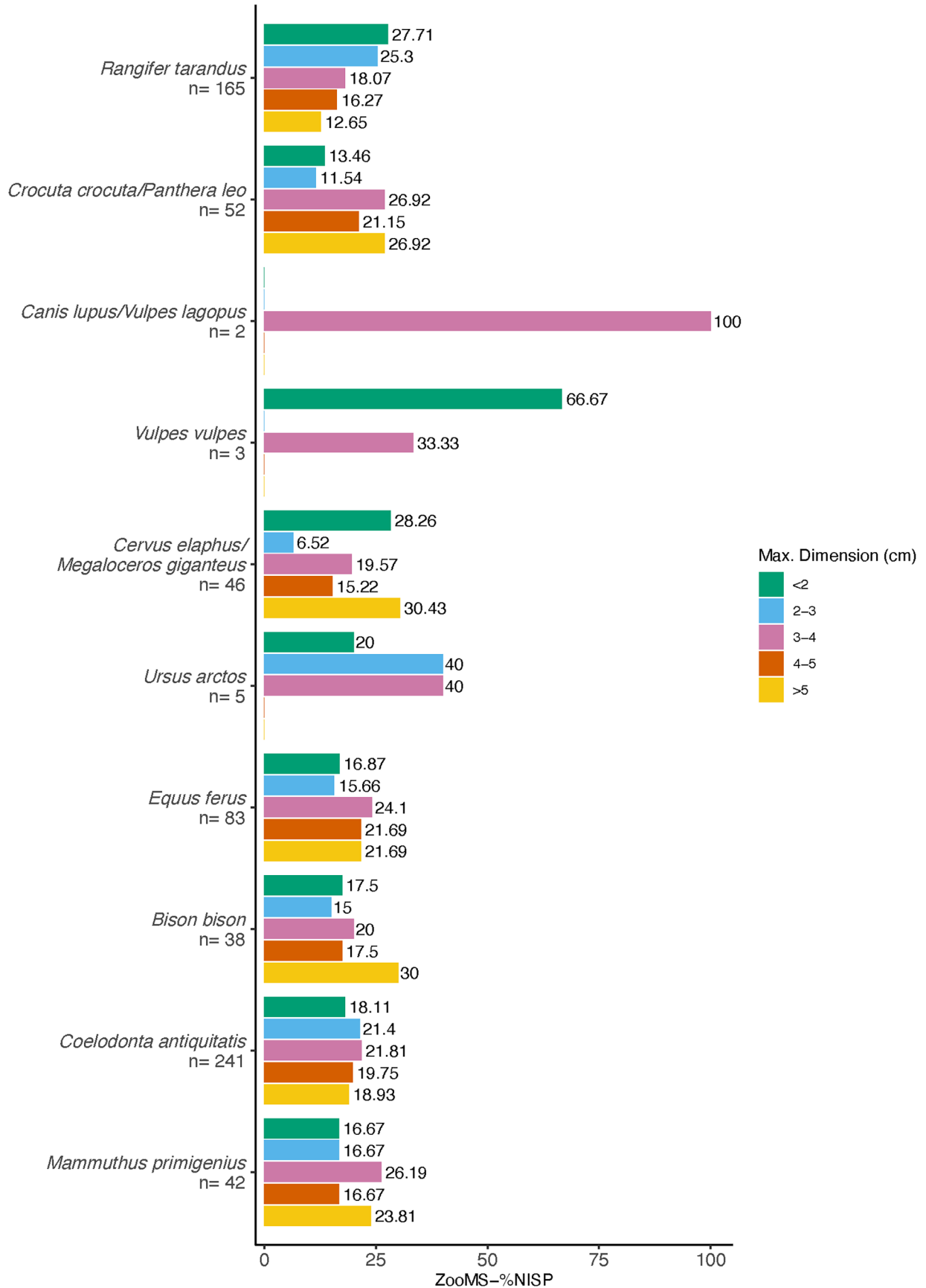


Figure 7. Percentage of number of ZooMS-identified specimens (ZooMS-%NISP) from Picken's Hole, Unit 3 (n=677; data from this study), according to taxon and fragment size.

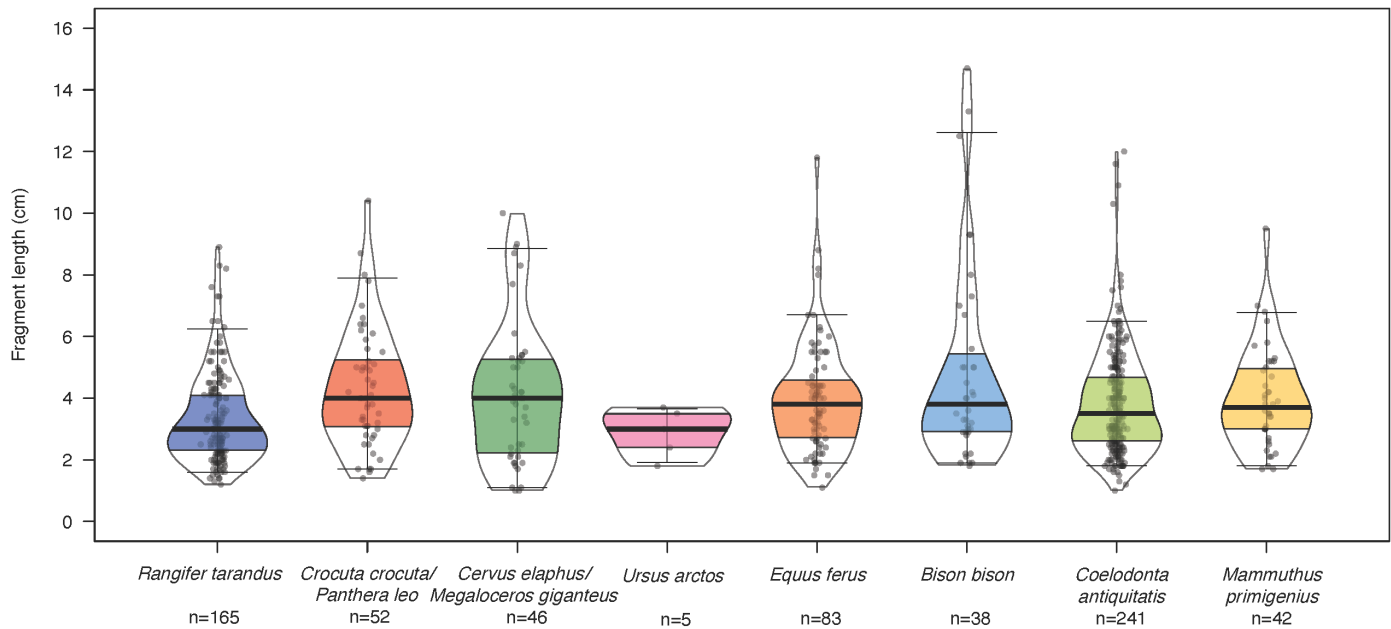


Figure 8. Distribution of fragment size for all ZooMS-identified taxa ( $n=672$ , excluding *Canis lupus/Vulpes lagopus* and *Vulpes vulpes* due to small sample sizes; data from this study) from Picken's Hole, Unit 3. The central black line is the median, the colored band is the interquartile range, and the T-bars are the 5th and 95th percentiles.

all other taxa. It is typically expected that species of different size would have different fragment size distributions (Lyman 1994; Reitz and Wing 2008), however, this does not appear to be the case for ZooMS identified fragments here and elsewhere (Discamps et al. 2024). The identification ratios suggest hyaena/lion, bison, and deer/giant deer have higher morphological identification rates than woolly rhinoceros, mammoth, and horse above, here their size distributions are indistinguishable from all taxa, except reindeer. So, although fragment length does not differ, identification rate does, meaning that horse is less anatomically identifiable than other similar sized taxa, which could be due to more intensive fragmentation, while woolly rhinoceros and mammoth are less anatomically identifiable perhaps due to their original body size, as would be expected (Morin 2012; Pickering et al. 2006). The smaller size of the anatomically unidentifiable reindeer fragments may also be an indication of more intensive fragmentation, though more data would be needed to assess this, such as morphological MNE and fragment lengths or weights (Discamps et al. 2024; Grayson 1984). Overall, differences in ZooMS-identified fragment size suggest that since morphological identification rates are linked to mammal size class and fragment length, then routes of fragmentation and varied taphonomic histories will affect the identification ratio.

#### SKELETAL/BODY PART REPRESENTATION

Comparison of skeletal/body part representation between morphology- and ZooMS-identified specimens facilitates the possible identification of morphologically invisible skeletal elements, which has implications for understand-

ing carcass transport and carnivore processing. Morphological dental remains are included here despite the 40 unidentified tooth fragments that were not analyzed using ZooMS (see Methods). Out of the 388 morphologically unidentifiable bone fragments analyzed using ZooMS that were assigned to bone element type, 95.6% ( $n=371$ ) produced a ZooMS identification. Of these, thorax fragments were most abundant (50.4%), followed by long bone fragments (46.9%), then antler/horn/tusk fragments (1.3%), cranial fragments (0.8%), and foot bone fragments (0.5%). This contrasts with the 988 morphological identifications, where dental remains were most dominant (71.4%), followed by foot bones (17.7%), limb bones (5.6%), cranial (3.1%), antler/horn/tusk fragments (2.3%), and thorax specimens (2.2%) (Figure 9; Supplementary Table S6).

Overall, dental remains and foot bones are most dominant in the morphological portion, while rib and long bone fragments dominate the ZooMS-identified portion. Woolly rhino, mammoth, horse, and bear are either solely or primarily represented by dentition in the morphological portion, while the ZooMS-identified portion includes rib, vertebrae, and long bone fragments. Woolly rhinoceros rib fragments and reindeer long bones are the most abundant ZooMS contributions (Figure 10; Supplementary Table S6). Scott (2018) suggests that the skeletal representation within the morphology-identified portion supports the primary accumulator being young hyaenas stealing jaws and relatively light limb bones from kill sites. Therefore, considering the quantification issues associated with rib and long bone fragments, where the NISP counts and faunal abundance are inflated, it appears that a proportion of post-cra-

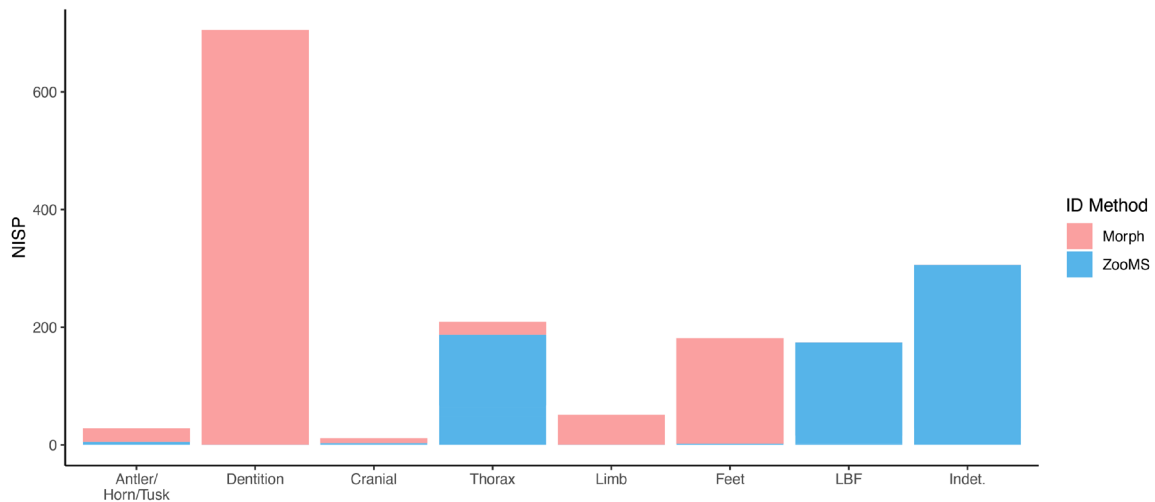


Figure 9. Number of identified specimens (NISP) by body part for all morphological ( $n=988$ ; data from Scott 2018) and ZooMS identified ( $n=677$ ; data from this study) taxa from Picken's Hole, Unit 3. Forty unidentified tooth fragments and 1441 unidentified indeterminate element fragments that were not identified for this study are not shown. Limb and feet bones are primarily identified morphologically, while LBF are solely identified using ZooMS.

nial body parts, which was fragmented to a morphologically unidentifiable point, was accumulating at the site.

### ZOOMS-IDENTIFIED TAPHONOMIC ANALYSIS

Several taphonomic observations of the ZooMS-identified portion were considered to explore accumulation dynamics (see Supplementary Materials for full data table). A detailed understanding of the taphonomic histories can rule out common causes of bone fracturing and establish what may be responsible for differential fragmentation and body part representation. Surface corrosion due to animal waste or burial environment was prevalent with observations for 94% of specimens covering from 10% to 100% surface area (Fernández-Jalvo and Andrews 2016). Plant root etching was observed on 77% of specimens as either light (62%) or heavy (15%), indicating that many specimens were in a plant-supporting sediment for some time during burial (Fernández-Jalvo and Andrews 2016; Macho-Callejo et al. 2023). While lithic refits indicate some horizontal movement (Wragg Sykes 2018), low levels of abrasion within the ZooMS-identified portion support minimal movement of the archaeological material. Abrasion was primarily either light (16%) or absent (74%), with 6% showing moderate abrasion and 4% with heavy abrasion. In addition, only 4% appear polished and no striations were observed. This suggests that the movement of faunal specimens within the sediment matrix, including via trampling, and exposure to fluvial- or aeolian-related abrasion was minimal (Fernández-Jalvo and Andrews 2016; Lyman 1994; Madgwick 2014), so abrasion can be ruled out as a major cause of fragmentation. The observed weathering stages were low overall, with none above Behrensmeyer stage 3, 'relatively heavy' (Behrensmeyer 1978) (Figure 10). Differences between the amount of light and moderately weathered specimens were suggested when tested using chi-squared

tests with adjusted residuals (Carlson 2017; Grayson and Delpech 2003; Ruebens et al, 2023) ( $\chi^2=122$ ,  $p<0.001$ ), likely caused by larger numbers of moderately weathered woolly rhinoceros and mammoth specimens, and larger numbers of lightly weathered reindeer specimens (Figure 11; Supplementary Table S7). While the length of fragments between light and moderate weathering was similar (Kolmogorov-Smirnov:  $D=0.09$ ,  $p=0.15$ ), fragments that were relatively heavily weathered were larger than those that display light ( $D=0.23$ ,  $p=0.004$ ) or moderate weathering ( $D=0.27$ ,  $p<0.001$ ) (Figure 12; Supplementary Table S8), therefore confirming that weathering does not explain fragmentation.

### Human Bone Surface Modification

While it was reported that no cut marks were visible on the morphological portion of the assemblage (Scott 2018), some possible human bone surface modifications were observed on 83 ZooMS-identified fragments (total  $n=708$ ) and 121 unanalyzed indeterminate bone fragments (total  $n=1441$ ) in this study (see Supplementary Table S9). Of the ZooMS-identified portion, taxa include woolly rhinoceros ( $n=32$ ), reindeer (13), horse (12), hyaena/lion (8), deer/giant deer (6), bison (5), mammoth (4), bear (2) and 1 failed ZooMS identification. These are 34 rib fragments, 30 indeterminate element fragments, 17 long bone fragments, 1 scapula and 1 vertebra. Modification types include potential burning ( $n=25$ ; Figure 13), cutmarks (1), hammerstone notches (6; includes one with possible cutmarks), and impact scars (61; including four with possible burning and five with possible hammerstone notches). The 121 observations on the unanalyzed portion include possible burning ( $n=33$ ), chop marks (1), and impact scars (90; includes two possible burning and one possible chop mark). Break morphology is mixed, with 8 fragments showing only fresh breaks, 122 with mixed fresh and dry breaks, and 74 showing dry breaks only. The total 204 bone fragments with observed



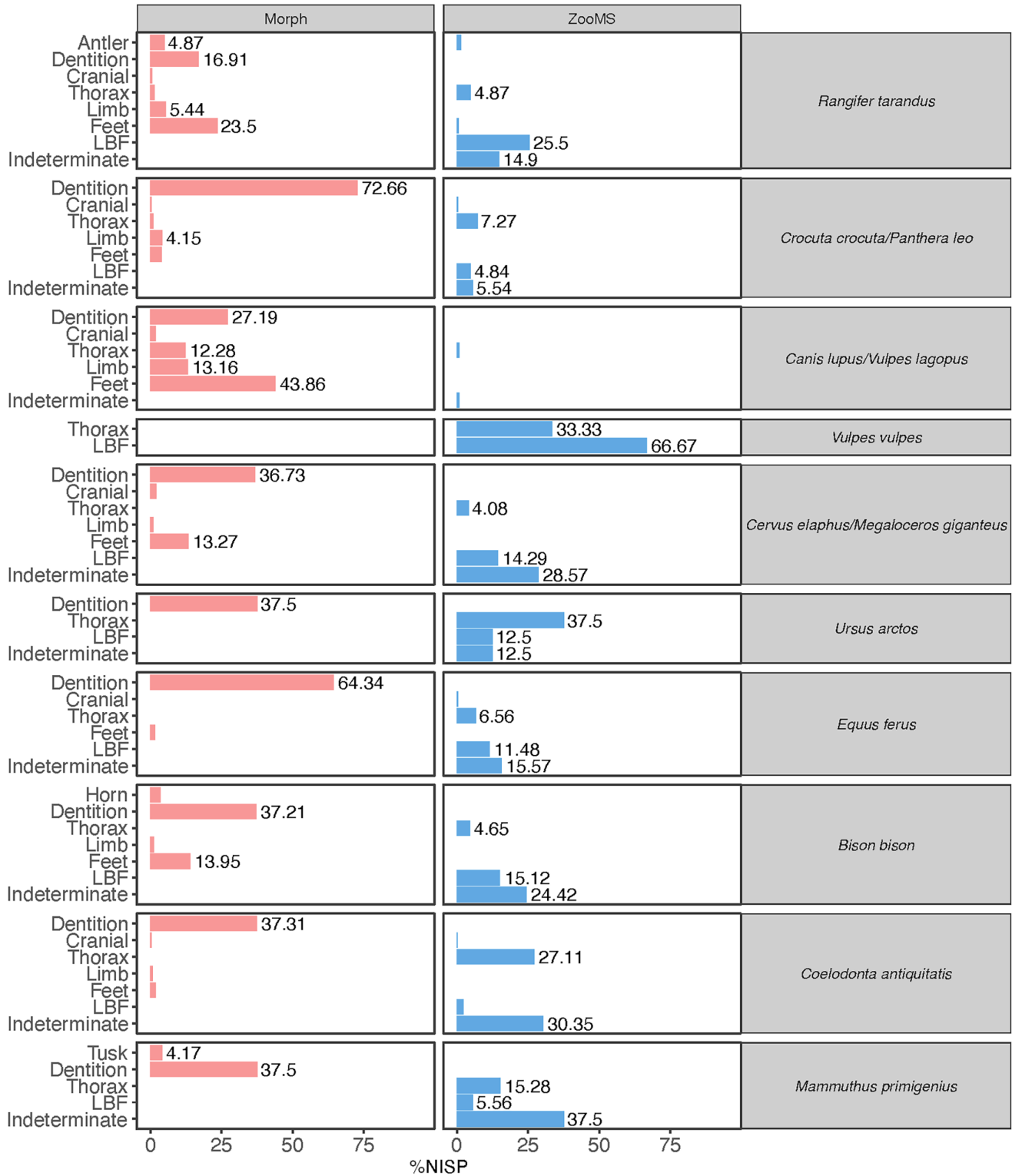


Figure 10. Percentage of number of identified specimens (%NISP) by body part across all morphological (n=988; data from Scott 2018) and ZooMS identified (n=677; data from this study) taxa from Picken's Hole, Unit 3. Note that mammoth and bear are represented solely by dentition within the morphological portion. Forty unidentified tooth fragments and 1441 unidentified indeterminate element fragments that were not identified for this study are not shown. Limb and feet bones are primarily identified morphologically, while LBF are solely identified using ZooMS.

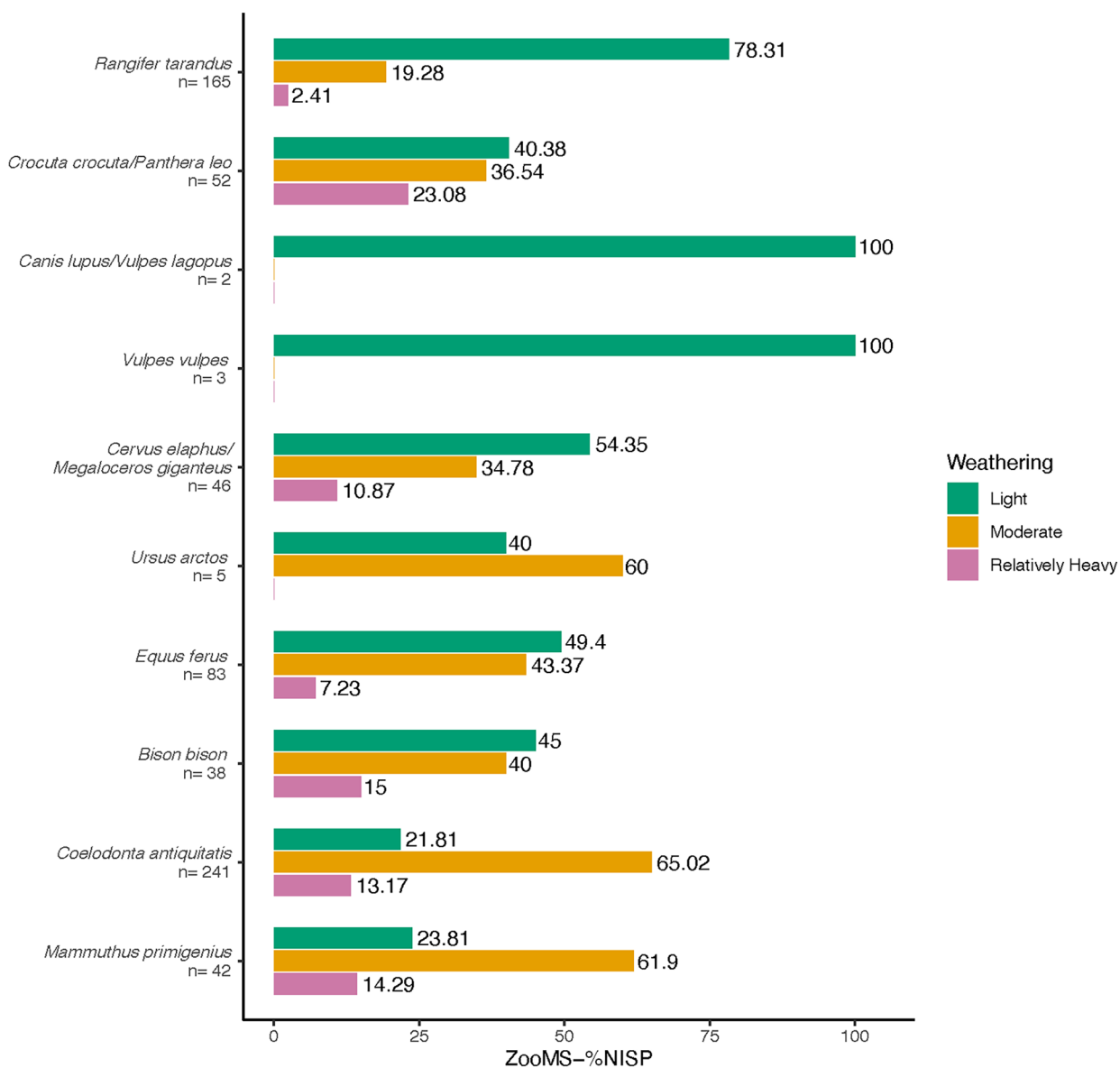


Figure 11. Percentage of number of ZooMS-identified specimens (ZooMS-%NISP) by weathering stage observations across ZooMS-identified taxa (n=677; data from this study) identified using ZooMS from Picken's Hole, Unit 3.

possible human modification include 153 with carnivore bone surface modification. These are 47 gnawed fragments that show possible burning (n=8) and impact scars (42; includes three with possible burning), and 106 fragments with signs of digestion and possible burning (41), impact scars (66; includes one possible burning and one possible chop mark). Fragments with observed modifications will undergo further assessment, such as viewing under magnification, to determine whether further investigation, such as SEM, is required. As such, study of these bone surface modifications is ongoing to conclusively establish whether they were caused by human activity.

### Carnivore Bone Surface Modification

Differences in carnivore bone surface modification (BSM) between taxa, fragment length, and skeletal/body part rep-

resentation were assessed to investigate differential fragmentation, carcass transport, and accumulation dynamics. Overall, the features of BSM caused by carnivore digestion and gnawing are consistent with common traits observed for bone specimens processed by modern spotted hyaena. For digestion, this includes significant acid etching, including acid-etched holes and edges that appear thinned (Figure 14), while extensive gnawing often created crenelated edges and gouging (Figure 15) (Haynes 1983; Mwebi and Brugal 2018; Sutcliffe 1970). There were similar patterns of carnivore BSM presence across all major taxa, except hyaena/lion, which had the opposite pattern to all others (see Figure 15). Woolly rhinoceros represents the largest proportion of digestion with 77% and 15% gnawing. Reindeer, deer/giant deer, and bison had comparable proportions with ~45–50% digestion and ~30% gnawing. By compari-

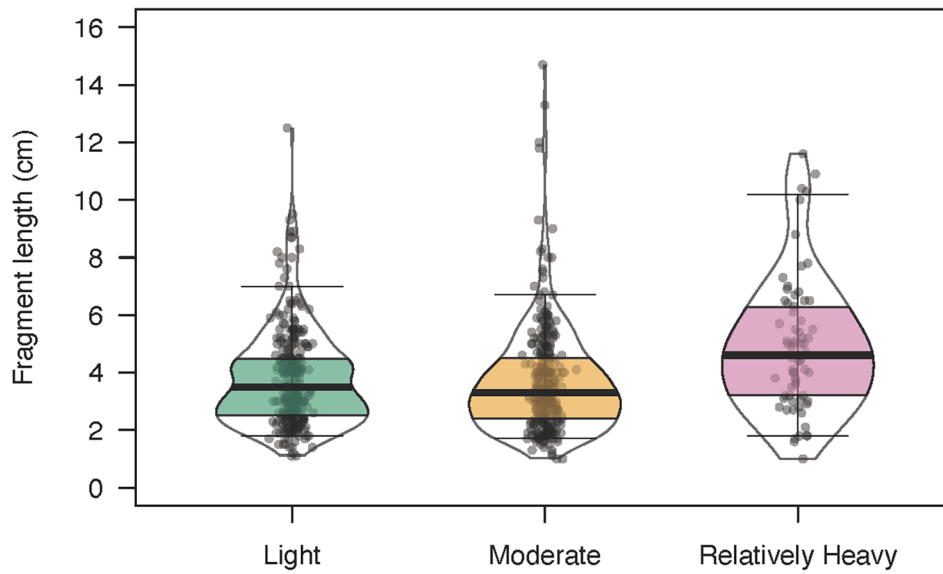


Figure 12. Distribution of fragment size according to weathering stage of all ZooMS-identified taxa ( $n=677$ ; data from this study) from Picken's Hole, Unit 3. The central black line is the median, the colored band is the interquartile range, and the T-bars are the 5th and 95th percentiles.



Figure 13. Unanalyzed indeterminate bone fragment with possible signs of burning from Picken's Hole, Unit 3.



Figure 14. ZooMS-identified horse long bone fragment with signs of digestion from Picken's Hole, Unit 3.



Figure 15. ZooMS-identified bison long bone fragment with signs of gnawing from Picken's Hole, Unit 3.

son, hyaena/lion specimens had 23% digestion and 35% gnawing. Since signs of digestion can override or negate gnaw marks, it might be expected that if there were high levels of digestion, there would be low levels of gnawing

(Binford 1981; Sutcliffe 1970). This was tested using composite chi-squared values with adjusted residuals, which suggests that there is a significant difference between the levels of gnawing and digestion ( $\chi^2=44$ ,  $p<0.001$ ). These



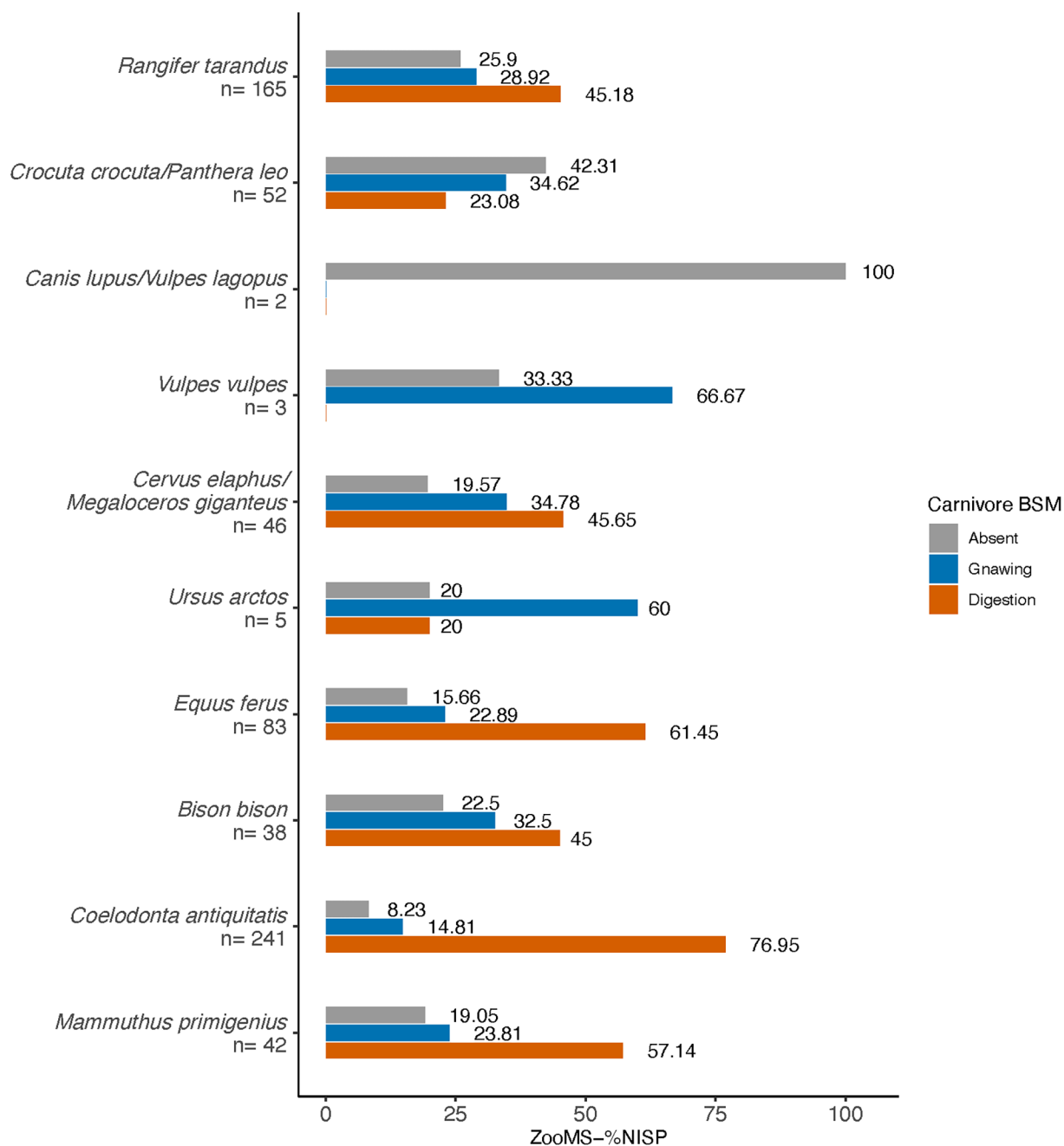


Figure 16. Percentage of number of ZooMS-identified specimens (ZooMS-%NISP) by carnivore bone surface modification observations across ZooMS-identified taxa (n=677; data from this study) from Picken's Hole, Unit 3.

differences were caused by an increase in gnaw marks for hyaena/lion, reindeer, and deer/giant deer specimens and an increase in digestion marks for woolly rhinoceros specimens (Figure 16; Supplementary Table S10). This suggests that hyaena/lion, reindeer, and deer/giant deer specimens were gnawed at the site and, if digested, the whole bone was not consumed, while woolly rhinoceros remains were often digested with little evidence of gnaw marks.

An examination of fragment length distribution using the Kolmogorov-Smirnov test (absent-digestion:  $D=0.21$ ,  $p<0.001$ ; gnawing-digestion:  $D=0.26$ ,  $p<0.001$ ) shows that

digested bone fragments were smaller than both gnawed fragments and fragments with no observed carnivore BSM (Figure 17; Supplementary Table S11). When taxon was controlled for, all taxa appeared to share this pattern, though only digested reindeer, horse, and woolly rhinoceros to a statistically significant level (Figure 18; Supplementary Table S12), likely due to their having the largest sample sizes.

A consideration of carnivore BSM and skeletal/body part representation allows for investigation of carcass transport and accumulation dynamics. Indeterminate fragments (those which cannot be assigned to a skeletal ele-

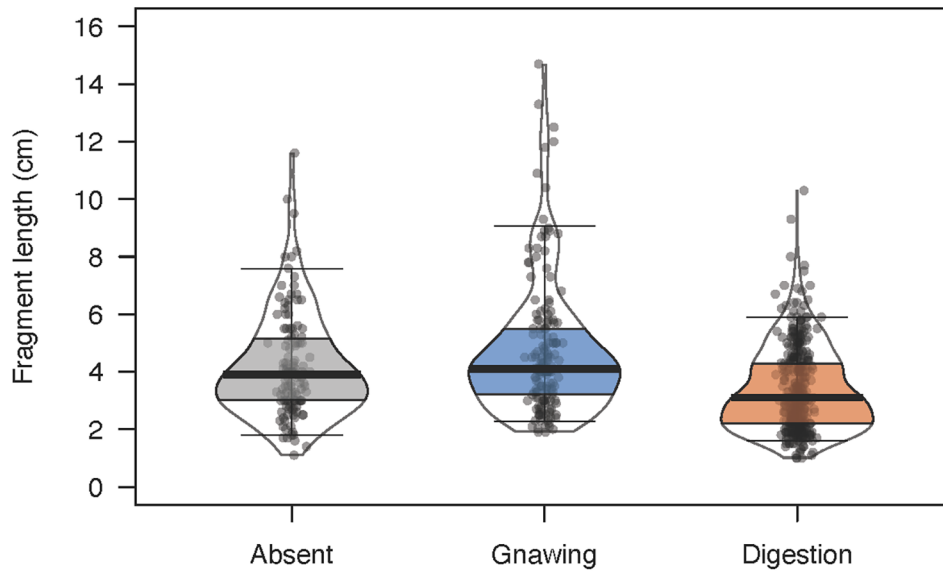


Figure 17. Distribution of fragment size according to carnivore bone surface modification observed on ZooMS-identified taxa ( $n=677$ ; data from this study) from Picken's Hole, Unit 3. The central black line is the median, the colored band is the interquartile range, and the T-bars are the 5th and 95th percentiles.

ment/body part) were included as they add value as an indication of fragmentation intensity and identifiability. While some taxa appear to have been consumed almost entirely with fragments often showing signs of digestion, other herbivores revealed more elements with gnaw marks. Taxa with similar identification ratios also had similar patterns of carnivore modifications, and similar skeletal/body part representation, suggesting these factors may be related. For the taxa with the fewest specimens identified morphologically—woolly rhinoceros, mammoth, and horse—these had the largest proportion of indeterminate fragments, ribs, and long bone fragments that showed signs of digestion in the ZooMS-identified component

(Figure 19; Supplementary Table S13). The high number of woolly rhinoceros fragments that the ZooMS method identified was dominated by digested specimens (primarily indeterminate [42.7%] and rib [33.6%] shaft fragments) with just a few gnawed fragments. This suggests that for the most part woolly rhinoceros carcasses were being consumed almost entirely and their remains were deposited at the site after passing through the digestive tract. A similar pattern holds for mammoth although a greater proportion of ribs (9.5%), long bones (4.8%), and indeterminate fragments (9.5%) have gnaw marks. This may be explained by the high proportion of juvenile teeth among the dentition of the morphologically identified component. If mammoth

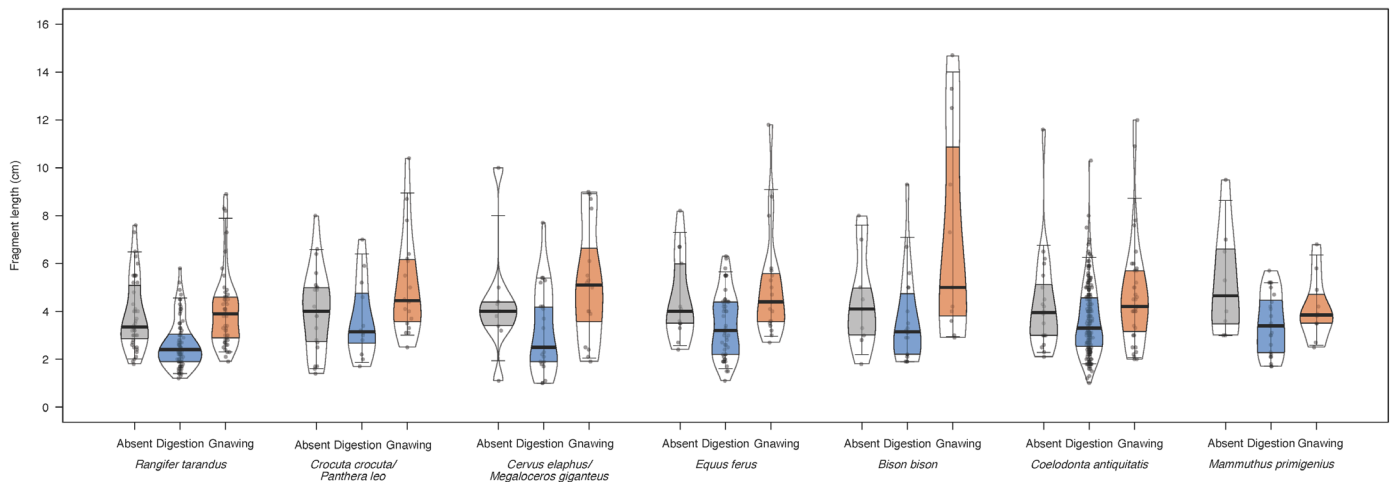


Figure 18. Fragment length distribution of carnivore bone surface modification observations across major ZooMS-identified taxa ( $n=667$ ; data from this study) from Picken's Hole, Unit 3. The central black line is the median, the colored band is the interquartile range, and the T-bars are the 5th and 95th percentiles.

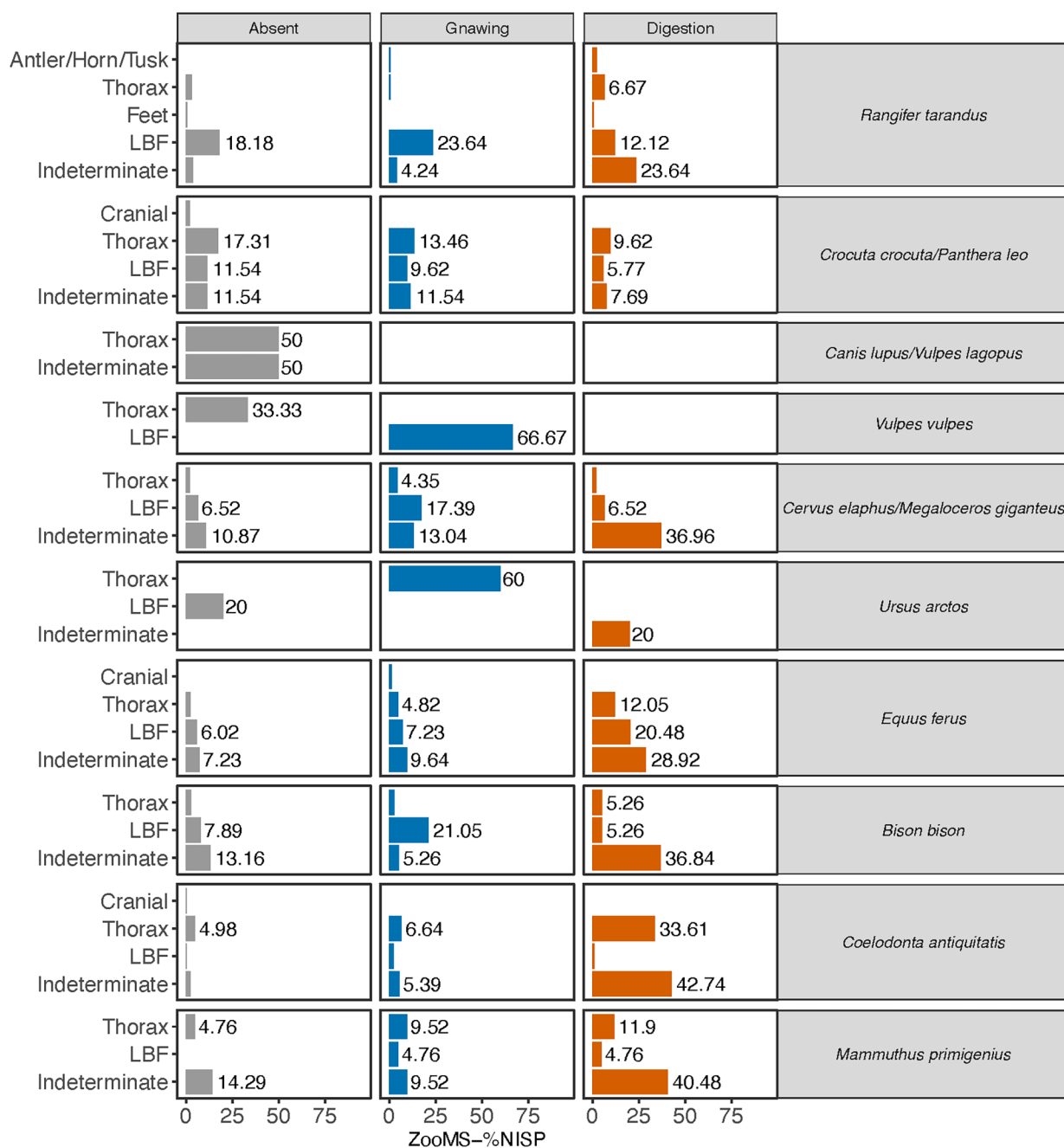


Figure 19. Percentage of number of ZooMS-identified specimens (ZooMS-%NISP) by body part and presence of carnivore bone surface modification across all ZooMS-identified taxa (n=677; data from this study) from Picken's Hole, Unit 3. Forty unidentified tooth fragments and 1441 unidentified indeterminate element fragments that were not identified for this study are not shown.

calves were targeted, then larger elements may have been available for transport to the den by younger hyaena and consumed there (Scott 2018; Sutcliffe 1970). Horse also had a similar pattern. Digested fragments make up the largest proportion of each body part represented, with fewer indeterminate (28.9%) fragments than woolly rhinoceros and mammoth, a similar proportion of rib (12%) fragments to mammoth, and more long bone (20.5%) fragments than either. The greater proportion of ZooMS-identified horse fragments identifiable to skeletal element/body part may be explained by the difference in size of these taxa, in that

fragments of a similar length that are able to be digested may be more identifiable for smaller taxa since a relatively greater proportion of the element is preserved. It appears that horse was also being consumed entirely, for the most part, with few elements left with gnaw marks. This pattern is not a result of abundance, since mammoth abundance is much lower than horse or woolly rhinoceros, therefore, it appears that the accumulation dynamics for woolly rhinoceros, horse, and mammoth remains were similar, and carnivore digestion appears largely responsible for their fragmentation. The herbivores with almost equal mor-

phology and ZooMS-identified representation—bison and deer/giant deer—had large proportions of indeterminate fragments showing signs of digestion (bison: 36%; deer/giant deer: 37%) and a greater proportion of long bone fragments with gnaw marks (bison: 21%; deer/giant deer: 17%). Therefore, bison and deer/giant deer may be mostly consumed, as with the taxa above, however, there were a greater number of specimens gnawed and not being digested, suggesting that carnivore digestion was responsible for some but not all fragmentation. The herbivore with the highest number of morphology-identified specimens, reindeer, had 23% digested indeterminate fragments and 23% gnawed long bone fragments. This was the lowest proportion of digested indeterminate fragments for the dominant herbivores, and the highest proportion of gnaw marked long bone fragments. This suggests that, despite their small size, carnivore digestion may not be solely responsible for reindeer fragmentation. This pattern of reindeer taphonomy may instead be due to carnivore gnawing that does not lead to digestion, such as when prey is more abundant and less of the carcass is consumed or more cub provisioning takes place where the bones are not completely digested. Absence of carnivore tooth marks on species that are consumed by hyaena is not evidence of absence since carnivore bone crushing may not leave any identifiable gnaw/tooth marks (Fourvel et al. 2015; Haynes, 1983; Lansing et al. 2009; Mwebi and Brugal 2018; Sutcliffe 1970).

The pattern for the carnivores was somewhat different, despite similarities in the identification ratio for hyaena/lion, bison, and deer/giant deer. Hyaena/lion specimens showed small proportions of digestion evidence across all body part categories (up to 10%), and larger proportions with gnawing (12%) or no evidence of carnivore activity (up to 15%). This may be a representative pattern of what remains after hyaena/lion consumption on-site, since the morphological analysis (Scott 2018) found that only old and young hyaena were present, likely representing individuals who had died in the den. While spotted hyaena only rarely attack and kill each other, they are known to consume clan members that die of natural causes (Kruuk 1972). Wolf/arctic fox specimens showed no evidence of carnivore activity. This suggests that these remains accumulated at the site not as carnivore prey and potentially when spotted hyaena were absent.

Within the ZooMS-identified portion there appears to be a relationship between ZooMS to Morph identification ratios, carnivore BSM, and skeletal/body part representation. Taxa with lower ZooMS to Morph identification ratios are represented by proportionately more digested fragments, while those with higher ratios have fewer digested remains and a greater number of elements with gnaw marks. This pattern suggests that carnivore digestion is responsible for lower levels of morphologically identifiable remains, while gnawing that does not lead to digestion and a smaller mammal size class mean higher anatomical identification rates.

## SUMMARY AND CONCLUSIONS

### THE ROLE OF CARNIVORES IN SITE FORMATION

Morphological to ZooMS identification ratio, carnivore BSM, and skeletal/body part representation appear to be linked. Lower identification ratios represent taxa with proportionately more digested fragments, while those with higher identification ratios have fewer digested remains and a greater number of elements with gnaw marks or unidentifiable carnivore BSM. Carnivore digestion is related to lower anatomical identification rates, while gnawing that does not lead to digestion, absence of carnivore activity, and smaller mammal size class were linked with higher anatomical identification rates. Modern spotted hyaena consume much of a carcass at the kill site, with little often brought back to the den amid fierce intra-clan competition, except during periods of high prey abundance when competition is less intense (Fourvel et al. 2015; Lansing et al. 2009). Therefore, it may be that the low identification ratio and high digestion presence for woolly rhinoceros, mammoth, and horse indicate stages where prey were primarily consumed during periods of intense intra-clan competition, while the middling identification ratio and high levels of digestion with increased gnaw mark presence on the bison and deer/giant deer indicate periods of relative prey abundance and some bone accumulation. The high identification ratio combined with lower digestion presence and higher gnaw mark presence for reindeer possibly indicates periods of high prey abundance meaning low intra-clan competition for food, and allowing more carcass remains to accumulate at the site (Figure 20). Despite similarities in the identification ratio with bison and deer/giant deer, hyaena/lion specimens showed small proportions of digestion evidence across all body part categories and larger proportions with gnawing or no evidence of carnivore activity, which may be an example of the pattern of remains that survive spotted hyaena consumption on-site, since these carcasses likely represent individuals that died and were consumed in the den (Kruuk 1972; Scott 2018; Sutcliffe 1970). With the highest identification ratio of all taxa, wolf/arctic fox specimens showed no evidence of carnivore activity, and no cut marks were found within the morphological component (Scott 2018), indicating that neither carnivore nor Neanderthal hunting behavior was likely responsible for their accumulation and that wolf/arctic fox may instead have used the cave when large carnivores were absent. Modern spotted hyaena move den sites regularly, using earthen dens as well as rock shelters, with occupation periods ranging from one week to eight months (Lansing et al. 2009). The ZooMS-identified grey wolf/arctic fox reveals their very high anatomical identification rate, and they appear to be present when spotted hyaena are absent, however, the ZooMS-identified sample size of two is problematic. Scott (2018) mentions that arctic fox could have been prey to either wolves or spotted hyaena but does not pres-



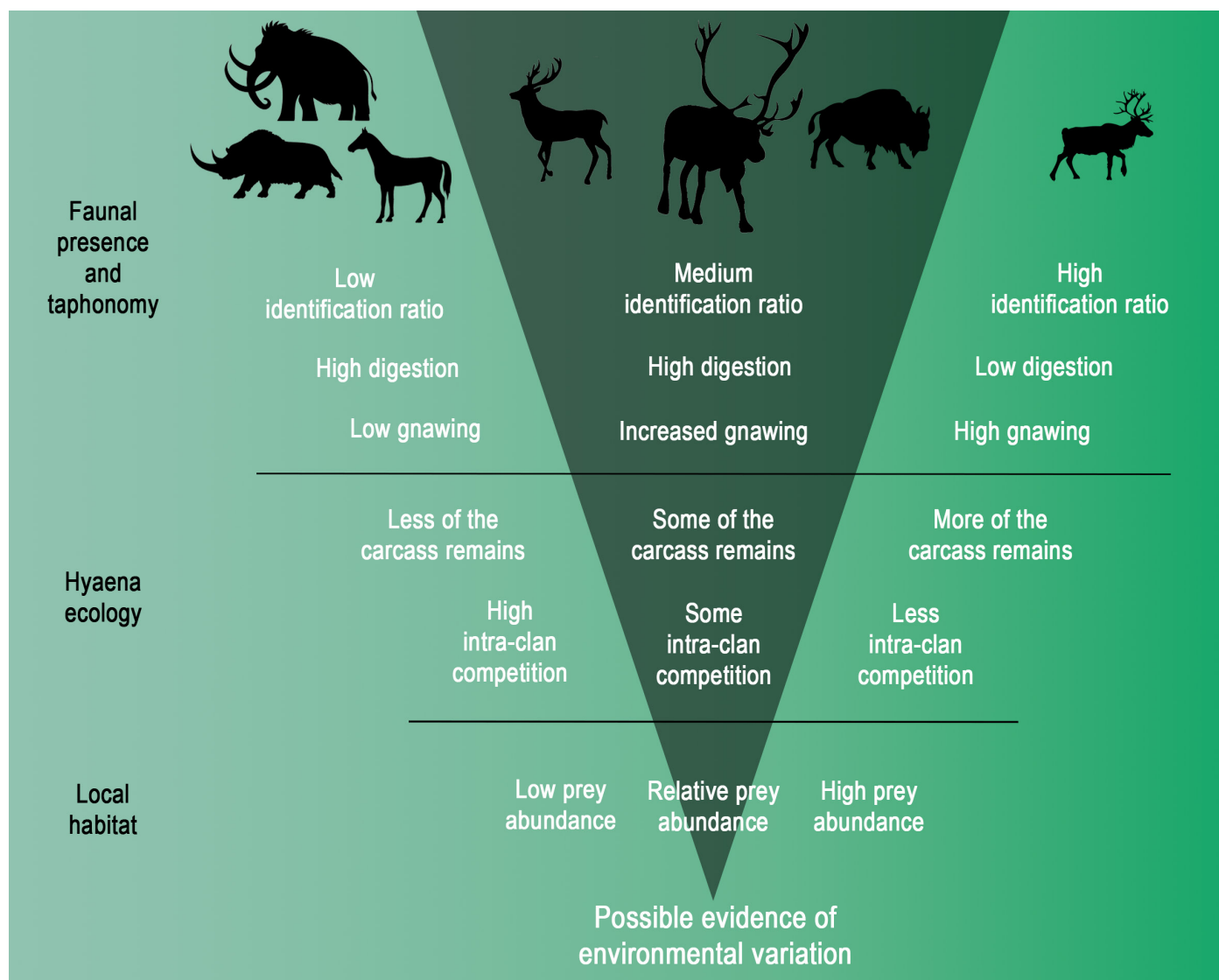


Figure 20. The distinct taphonomic patterns found for woolly rhinoceros, mammoth and horse remains, deer/giant deer and bison remains, and reindeer remains may be a result of hyaena behaviors and reflect variation in prey availability and the local habitat spanning tens of thousands of years.

ent any taphonomic evidence. It may also be possible that due to stratigraphic issues, the grey wolf/arctic fox remains may originate from Unit 5, when the site was primarily a wolf den (Scott 2018), although arctic fox was consistently identified during the excavation of Unit 3 (P.L. Smart, personal communication). The ZooMS-identified addition of red fox to the faunal presence represents another carnivore competing for resources, though taphonomy suggests they were processed by carnivores. Although spotted hyaena were the primary accumulators at Picken's Hole, wolves, red fox, and arctic fox may also have contributed. The presence of gnawing only on the red fox specimens could suggest they were processed by a carnivore other than hyaena, though, again, the small sample size is problematic.

#### ECOLOGICAL RECONSTRUCTION AND NEANDERTHAL BEHAVIOR

The small lithic assemblage from Picken's Hole indicates it is likely to have been a rare task site used for the primary stages of lithic tool manufacture. The limited lithics, along with lack of confirmed human bone surface modifications on the morphological and ZooMS-identified fauna and the absence of Neanderthals in the species identified through ZooMS supports previous suggestions that the site may have only been used by Neanderthals on a handful of occasions (Wragg Sykes 2018). The identification of red fox through ZooMS adds to the number of carnivores that were operating alongside Neanderthals in the local landscape and with whom Neanderthals were competing

for resources and natural shelter. The taphonomy of the ZooMS-identified portion suggests that grey wolf/arctic fox were present at the site when other predators were not (this study; Scott 2018). Though Neanderthals were present more broadly in the region, with larger occupation sites within 10–20km (Jacobi 2000; Jacobi et al. 2006; Wragg Sykes 2018), the ZooMS-identified species and taphonomy confirms Picken's Hole was primarily occupied by carnivores, particularly hyaenas. The limited evidence of Neanderthals' use of the cave, along with the abundance of evidence indicating carnivore use suggests that Neanderthals may have avoided prolonged use of the cave because of the presence of carnivores but co-existed with them in the wider landscape.

### BENEFITS OF INVESTIGATING ZOOMS-IDENTIFIED BONE FRAGMENTS AT PICKEN'S HOLE

The inclusion of ZooMS-identified specimens supports Scott's (1986; 2018) assessment of Picken's Hole as primarily a hyaena den but adds visibility of the post-cranial skeleton and differences in taphonomic history between species. Specifically, that along with high representation from anatomically identified dentition, the post-cranial elements of key prey species were present at the site and subjected to varied intensities of carnivore processing. Woolly rhinoceros, horse, and mammoth were perhaps exploited under potentially intense intra-clan competition, while deer/giant deer and bison were less intensively processed, and reindeer even less still, suggesting more bone accumulated at the site during periods of greater prey abundance. These differences may represent an averaged variability in prey abundance, and therefore seasonal or environmental changes, which is not visible from the morphological component alone. The environment, prey availability, and clan size are known to affect spotted hyaena bone accumulation at den sites today. Making a direct comparison of Pleistocene hyaena ecology with modern hyaena is potentially limited, however, it appears likely that the hyaena-made bone accumulations at Picken's Hole, Unit 3, occurred over tens of thousands of years during repeat occupations. Variation in prey abundance and hyaena bone accumulation rates were thus likely averaged over significant time periods, therefore, these patterns in fragmentation and carnivore BSM revealed by ZooMS analysis may represent seasonal variation or broader climatic and environmental change (Lansing et al. 2009; Mwebi and Brugal 2018). To investigate whether accumulations occurred during mild or cooler periods further work is required, such as stable isotope analysis (Hedges et al. 2004; Stevens et al. 2021). ZooMS-identified fragments also reveal the presence of other carnivore species that do not appear intensively processed by spotted hyaena and so adds nuance to understanding the presence of multiple carnivore species at the site during the accumulation of Unit 3 and the impact of this for Neanderthal use of the cave. Further work on the Picken's Hole faunal assemblage such as the inclusion of morphological MNE and specimen lengths or weights

would provide greater detail on fragmentation rates, while morphological taphonomy data would facilitate comparison with the ZooMS-identified taphonomy and provide clarity on causes of fragmentation. Detailed investigation of possible human bone surface modifications on several ZooMS-identified fragments is ongoing and may provide further information on whether Neanderthal site-use included subsistence behavior. Stable isotope analysis on ZooMS-identified bone fragments is also ongoing to explore the local climate and isotopic food web and further understand the ecology of Neanderthal groups operating in the wider landscape.

### ACKNOWLEDGMENTS

FH was supported by an AHRC studentship (studentship reference: 16137110). We would like to thank the University of Bristol Speleological Society Museum for granting access to the Picken's Hole faunal collections, and Graham Mullan and Pete Smart for valuable input on the final draft. We would also like to thank the UCL undergraduate and post-graduate student volunteers who assisted with the initial sampling of the over 2000 bone fragments: Valentina Arroyave, Shu Chung, Elizabeth Church, Hanwen Cao, Ellie Crew, Yunqi Deng, Toby Fetterlein, George Ferguson, Juliet Fynn, Maura Griffith, Helen Hampton, Amy Hutton, Megan Hinks, Mathieu Isbell, Ariel Jin, Mark Johnson, Giselle Kiraly, Sheridan Lea, Isla Lury, Florence Marsden, Gwendoline Maurer, Thomas Mumelter, Iqra Mirza, Marie Middleton, Iris Oliveira, Catherine Pavitt, Ines Phillipson, Alexandra Poulter, Rhonda Prout, Roberto Ragno, Jyothi Sadeh, Chloe South, Anastasia Solomou, Anthony Teis, Paul Tulomba, Ariel Twan, Meng Zhang, Xuezhong Zhao, and Jingyuan Zou.

### DATA AVAILABILITY

Supplementary data for this manuscript is available through Zenodo. This includes the supplementary tables (SI #1), R scripts and data for the figures, tables, and statistical tests (SI #2), and the R scripts and MALDI output (.mzml) files used for processing ZooMS spectra (SI #3).



This work is distributed under the terms of a [Creative Commons Attribution-NonCommercial 4.0 Unported License](https://creativecommons.org/licenses/by-nc/4.0/).

### REFERENCES

- Aldhouse-Green, S., Scott, K., Schwarcz, H.P., Grün, R., Housley, R.A., Rae, A., Bevins, R., and Redknap, M., 1995. Coygan Cave, Laugharne, South Wales, a Moustertian site and hyaena den: a report on the University of Cambridge excavations. *Proc. Prehist. Soc.* 61, 37–79.
- Andrews, P., Cook, J., 1990. *Owls, Caves and Fossils: Predation, Preservation, and Accumulation of Small Mammal Bones in Caves, With an Analysis of the Pleistocene Cave Faunas from Westbury-sub-Mendip, Somerset, UK.* University of Chicago Press, Chicago.
- ApSimon, A.M., Mullan, G.J., Smart, P.L., 2018. Introduction to the 1960's excavation at Picken's Hole. *Proc.*

- Univ. Bristol Spealaeol. Soc. 27(3), 239–244.
- Apsimon, A.M., and Smart, P.L., 2018. The stratigraphy of the deposits in Picken's Hole. *Proc. Univ. Bristol Spealaeol. Soc.* 27(3), 245–259.
- Ashton, N., Scott, B., 2016. The British Middle Palaeolithic. *Quatern. Int.* 411, 62–76. <https://doi.org/10.1016/j.quaint.2015.06.011>
- Balch, H.E., 1947. *The Mendip Caves*. Butterworth-Heinemann, Bristol.
- Behrensmeier, A.K., 1978. Taphonomic and ecologic information from bone weathering. *Paleobiology* 4(2), 150–162. <http://www.jstor.org/stable/2400283>
- Binford, L.R., 1981. *Bones: Ancient Men and Modern Myths*. Academic Press, New York.
- Bond, C.J., 2004. The supply of raw materials for later prehistoric stone tool assemblages and the maintenance of memorable places in central Somerset. In: Walker, E.A., Wenban-Smith, F.F., Healy, F.M. (Eds.), *Lithics in Action. Papers from the Conference Lithic Studies in the Year 2000*. Lithic Studies Society Occasional Papers 8. Oxbow Books, Oxford, 128–143.
- Buckley, M., Collins, M., Thomas-Oates, J., Wilson, J.C., 2009. Species identification by analysis of bone collagen using matrix-assisted laser desorption/ionisation time-of-flight mass spectrometry. *Rapid Commun. Mass Spectrom.* 23, 3843–3854. <https://doi.org/10.1002/rcm>
- Bunn, H.T., Kroll, E.M., Ambrose, S.H., Behrensmeier, A.K., Binford, L.R., Blumenshine, R.J., Klein, R.G., McHenry, H.M., O'Brien, C.J., and Wymer, J.J., 1986. Systematic butchery by Plio/Pleistocene hominids at Olduvai Gorge, Tanzania [and Comments and Reply]. *Curr. Anthropol.*, 27(5), 431–452. <https://doi.org/10.1086/203467>
- Campbell, J.B., and Sampson, C.G., 1971. *A New Analysis of Kent's Cavern*, Devonshire, England. University of Oregon Anthropological Papers 3, 1–40.
- Cannon, M.D., 2013. NISP, bone fragmentation, and the measurement of taxonomic abundance. *J. Archaeol. Method Theory*, 20(3), 397–419. <https://doi.org/10.1007/s10816-012-9166-z>
- Carlson, D.L., 2017. *Quantitative Methods in Archaeology using R*. Cambridge University Press, Cambridge, UK.
- Currant, A.P., Jacobi, R., 2011. The mammal faunas of the British late Pleistocene. *Develop. Quatern. Sci.* 14, 165–180. <https://doi.org/10.1016/B978-0-444-53597-9.00010-8>
- Dansgaard, W., Johnsen, S.J., Clausen, H.B., Dahl-Jensen, D., Gundestrup, N.S., Hammer, C.U., Hvidberg, C.S., Steffensen, J.P., Sveinbjörnsdóttir, A.E., Jouzel, J., Bond, G., 1993. Evidence for general instability of past climate from a 250-kyr ice-core record. *Nature* 364(6434), 218–220. <https://doi.org/10.1038/364218a0>
- Discamps, E., Karen, R., Smith, G.M., Hublin, J.-J., 2024. Can ZooMS help assess species abundance in highly fragmented bone assemblages? Integrating morphological and proteomic identifications for the calculation of an adjusted ZooMS-eNISP. *PaleoAnthropology* 2024:2, 282–297.
- Egeland, A.G., Egeland, C.P., Bunn, H.T., 2008. Taphonomic analysis of a modern spotted hyena (*Crocuta crocuta*) den from Nairobi, Kenya. *J. Taphonomy* 6, 275–299.
- Fernández-Jalvo, Y., Andrews, P., 2016. *Atlas of Taphonomic Identifications. Vertebrate Paleobiology and Paleoanthropology*. Springer, Dordrecht. <https://doi.org/10.1007/978-94-017-7432-1>
- Fisher, J.W., 1995. Bone surface modifications in zooarchaeology. *J. Archaeol. Method Theory* 2(1), 7–68. <https://doi.org/10.1007/BF02228434>
- Fourvel, J.B., Fosse, P., Avery, G., 2015. Spotted, striped or brown? Taphonomic studies at dens of extant hyaenas in eastern and southern Africa. *Quatern. Int.*, 369, 38–50. <https://doi.org/10.1016/j.quaint.2014.08.022>
- Gibb, S., Strimmer, K., 2012. Maldiquant: a versatile R package for the analysis of mass spectrometry data. *Bioinformatics* 28(17), 2270–2271. <https://doi.org/10.1093/bioinformatics/bts447>
- Gifford-Gonzalez, D., 2018. Reasoning with zooarchaeological counting units and statistics. In *Introduction to Zooarchaeology*. Springer International Publishing, Cham, pp. 385–412. [https://doi.org/https://doi.org/10.1007/978-3-319-65682-3\\_18](https://doi.org/https://doi.org/10.1007/978-3-319-65682-3_18)
- Grayson, D.K., 1984. *Quantitative Zooarchaeology*. Academic Press, London. <https://doi.org/10.1016/c2009-0-21855-1>
- Grayson, D.K., Delpech, F., 2003. Ungulates and the Middle-to-Upper Paleolithic transition at Grotte XVI (Dordogne, France). *J. Archaeol. Sci.*, 30(12), 1633–1648. [https://doi.org/10.1016/S0305-4403\(03\)00064-5](https://doi.org/10.1016/S0305-4403(03)00064-5)
- Guthrie, R.D., 1982. Mammals of the mammoth steppe as paleoenvironmental indicators. In: Hopkins, D.M., Matthews, J.V., Schweger, C.E. (Eds.), *Paleoecology of Beringia*. Academic Press, New York, pp. 307–326. <https://doi.org/10.1016/b978-0-12-355860-2.50030-2>
- Harrison, R.A., 1977. The Uphill Quarry Caves, Weston-super-Mare, a reappraisal. *Proc. Univ. Bristol Speleol. Soc.* 14, 233–254.
- Haynes, G., 1983. A guide for differentiating mammalian carnivore taxa responsible for gnaw damage to herbivore limb bones. *Paleobiology* 9(2), 164–172. <https://doi.org/10.1017/S0094837300007545>
- Hedges, R.E.M., Stevens, R.E., Richards, M.P., 2004. Bone as a stable isotope archive for local climatic information. *Quatern. Sci. Rev.*, 23(7–8), 959–965. <https://doi.org/10.1016/j.quascirev.2003.06.022>
- Hibbert, D., 1982. History of the Steppe-Tundra Concept. In: Hopkins, D.M., Matthews, J.V., Schweger, C.E. (Eds.), *Paleoecology of Beringia*. Academic Press, New York, pp. 153–156. <https://doi.org/10.1016/b978-0-12-355860-2.50017-x>
- Higham, T.F.G., Jacobi, R., Bronk Ramsey, C., 2006. AMS radiocarbon dating of ancient bone using ultrafiltration. *Radiocarbon* 48, 179–195. <https://doi.org/10.1017/S0033822200066388>
- Holloran, F., 2024. Picken's Hole. PDF map. Scale 1:5000. OS MasterMap. Ordnance Survey using Digimap Ordnance Survey Collection. <https://digimap.edina.ac.uk>



Created 1st February 2024.

- Jacobi, R., 2000. The Late Pleistocene archaeology of Somerset. In: Webster, C. (Ed.), *Somerset Archaeology: Papers to Mark 150 Years of the Somerset Archaeological and Natural History Society*. Somerset County, Taunton, pp. 45–52.
- Jacobi, R., 2004. Some observations on the non-flint lithics from Creswell Crags. *Lithics* 25, 39–64. <http://journal.lithics.org/index.php/lithics/article/view/431>
- Jacobi, R., Higham, T.F.G., Bronk Ramsey, C., 2006. AMS radiocarbon dating of Middle and Upper Palaeolithic bone in the British Isles: improved reliability using ultrafiltration. *J. Quatern. Sci.* 21(5), 557–573. <https://doi.org/10.1002/jqs.1037>
- Jacobi, R., Rose, J., MacLeod, A., Higham, T.F.G., 2009. Revised radiocarbon ages on woolly rhinoceros (*Coelodonta antiquitatis*) from western central Scotland: significance for timing the extinction of woolly rhinoceros in Britain and the onset of the LGM in central Scotland. *Quatern. Sci. Rev.* 28(25–26), 2551–2556. <https://doi.org/10.1016/j.quascirev.2009.08.010>
- Kahlke, R.D., 2014. The origin of Eurasian mammoth faunas (*Mammuthus-Coelodonta* faunal complex). *Quatern. Sci. Rev.* 96, 32–49. <https://doi.org/10.1016/j.quascirev.2013.01.012>
- Klein, R.G., Cruz-Uribe, K., 1984. *The Analysis of Animal Bones From Archeological Sites*. University of Chicago Press, Chicago.
- Kruuk, H., 1972. *The Spotted Hyaena*. University of Chicago Press, Chicago.
- Langford, H.E., Boreham, S., Briant, R.M., Coope, G.R., Horne, D.J., Schreve, D.C., Whittaker, J.E., Whitehouse, N.J., 2014. Middle to Late Pleistocene palaeoecological reconstructions and palaeotemperature estimates for cold/cool stage deposits at Whittlesey, eastern England. *Quatern. Int.* 341, 6–26. <https://doi.org/10.1016/j.quaint.2014.01.037>
- Lansing, S.W., Cooper, S.M., Boydston, E.E., Holekamp, K.E., 2009. Taphonomic and zooarchaeological implications of spotted hyena (*Crocuta crocuta*) bone accumulations in Kenya: a modern behavioral ecological approach. *Paleobiology* 35(2), 289–309. <https://doi.org/10.1666/08009.1>
- Le Meillour, L., Sinet-Mathiot, V., Ásmundsdóttir, R.D., Hansen, J., Mylopotamitaki, D., Troché, G., Xia, H., Herrera Bethencourt, J., Ruebens, K., Smith, G.M., Fagnäs, Z., Welker, F., 2024. Increasing sustainability in palaeoproteomics by optimizing digestion times for large-scale archaeological bone analyses. *IScience* 27(4), 109432. <https://doi.org/10.1016/j.isci.2024.109432>
- Lewis, S.G., Maddy, D., Buckingham, C., Coope, G.R., Field, M.H., Keen, D.H., Pike, A.W.G., Roe, D. A., Scaife, R.G., Scott, K., 2006. Pleistocene fluvial sediments, palaeontology and archaeology of the upper River Thames at Latton, Wiltshire, England. *J. Quatern. Sci.* 21(2), 181–205. <https://doi.org/10.1002/jqs.958>
- Lyman, R.L., 1994. *Vertebrate Taphonomy*. Cambridge University Press, Cambridge, UK.
- Lyman, R.L., Wolverton, S., 2023. Quantification in zooarchaeology and palaeoethno(archaeo)botany. In: Pollard, A.M., Armitage, R.A., Makarewicz, C.A. (Eds.), *Handbook of Archaeological Sciences* (2nd edition). John Wiley & Sons, Hoboken, NJ, pp. 1211–1226. <https://doi.org/https://doi.org/10.1002/9781119592112.ch60>
- Macho-Callejo, A., García-Morato, S., Gutiérrez, A., Marin-Monfort, D., Fernández-Jalvo, Y., 2023. Put down roots and find the plant!: preliminary results of root etching and its implications. *Hist. Biol.*, 1–9. <https://doi.org/10.1080/08912963.2023.2263865>
- Madgwick, R., 2014. What makes bones shiny? Investigating trampling as a cause of bone abrasion. *Archaeol. Anthropol. Sci.* 6(2), 163–173. <https://doi.org/10.1007/s12520-013-0165-0>
- Marra, A.C., 2013. Evolution of endemic species, ecological interactions and geographical changes in an insular environment: a case study of Quaternary mammals of Sicily (Italy, EU). *Geosciences (Switzerland)* 3(1), 114–139. <https://doi.org/10.3390/geosciences3010114>
- Martisius, N.L., Welker, F., Dogandžić, T., Grote, M.N., Rendu, W., Sinet-Mathiot, V., Wilcke, A., McPherron, S.J.P., Soressi, M., Steele, T.E., 2020. Non-destructive ZooMS identification reveals strategic bone tool raw material selection by Neandertals. *Sci. Rep.* 10(1), 1–12. <https://doi.org/10.1038/s41598-020-64358-w>
- Mellars, P.A., 1996. *The Neanderthal Legacy. An Archaeological Perspective from Western Europe*. Princeton University Press, Princeton, NJ. [https://doi.org/10.1016/s0160-9327\(97\)88950-8](https://doi.org/10.1016/s0160-9327(97)88950-8)
- Meloro, C., Raia, P., Barbera, C., 2007. Effect of predation on prey abundance and survival in Plio-Pleistocene mammalian communities. *Evol. Ecol. Res.* 9(3), 505–525.
- Morin, E., 2012. *Reassessing Paleolithic Subsistence: The Neandertal and Modern Human Foragers of Saint-Césaire*. Cambridge University Press, Cambridge, UK.
- Morin, E., Ready, E., Boileau, A., Beauval, C., Coumont, M.-P., 2017. Problems of identification and quantification in archaeozoological analysis, part II: presentation of an alternative counting method. *J. Archaeol. Method Theory* 24, 938–973.
- Mullan, G.J., 2018. Radiometric dating of samples from Picken’s Hole. *Proc. Univ. Bristol Spealaeol. Soc.* 27(3), 261–265.
- Mwebi, O., Brugal, J.P., 2018. Comparative taphonomical studies of sympatric hyenids (*Crocuta crocuta* and *Hyaena hyeana*) bone assemblages, insights from modern dens in Kenya. *Quaternaire* 29(1), 13–20. <https://doi.org/10.4000/quaternaire.8563>
- Orton, D.C., 2012. Taphonomy and interpretation: an analytical framework for social zooarchaeology. *Int. J. Osteoarchaeol.* 22(3), 320–337. <https://doi.org/10.1002/oa.1212>
- Pengelly, W., 1873. The cavern discovered in 1858 at Windmill Hill, Brixham, South Devon. *Trans. Devonshire Assoc. Advance. Sci. Lit. Art* 6, 775–856.
- Pengelly, W., 1884. *The literature of Kent’s Cavern, part V.*



- Trans. Devonshire Assoc. 14, 189–343.
- Pettitt, P., White, M., 2012. The British Palaeolithic: Hominin Societies at the Edge of the Pleistocene World. Routledge, London. <https://doi.org/10.4324/9780203141441>
- Pickering, T.R., Egeland, C.P., Schnell, A.G., Osborne, D.L., Enk, J., 2006. Success in identification of experimentally fragmented limb bone shafts: implications for estimates of skeletal element abundance in archaeofaunas. *J. Taphonomy* 4(2), 97–108. <http://digitalcommons.unl.edu/anthropologyfacpub/31/>
- Prendergast, M.E., Domínguez-Rodrigo, M., 2008. Taphonomic analyses of a hyena den and a natural-death assemblage near Lake Eyasi (Tanzania). *J. Taphonomy* 6(3–4), 301–335.
- Proctor, C.J., Collcutt, S.N., Currant, A.P., Hawkes, C.J., Roe, D.A., Smart, P.L., 1996. A report on the excavations at Rhinoceros Hole, Wookey. *Proc. Univ. Bristol Spelaeol. Soc.* 20(3), 237–262. <https://doi.org/10.1080/21622965.2013.802649>
- Rasmussen, S.O., Bigler, M., Blockley, S.P., Blunier, T., Buchardt, S.L., Clausen, H.B., Cvijanovic, I., Dahl-Jensen, D., Johnsen, S.J., Fischer, H., Gkinis, V., Guillevic, M., Hoek, W.Z., Lowe, J.J., Pedro, J.B., Popp, T., Seierstad, I.K., Steffensen, J.P., Svensson, A.M., ... Winstrup, M., 2014. A stratigraphic framework for abrupt climatic changes during the Last Glacial period based on three synchronized Greenland ice-core records: refining and extending the INTIMATE event stratigraphy. *Quatern. Sci. Rev.* 106, 14–28. <https://doi.org/10.1016/j.quascirev.2014.09.007>
- Reimer, P.J., Austin, W.E.N., Bard, E., Bayliss, A., Blackwell, P.G., Bronk Ramsey, C., Butzin, M., Cheng, H., Edwards, R.L., Friedrich, M., Grootes, P.M., Guilderson, T.P., Hajdas, I., Heaton, T.J., Hogg, A.G., Hughen, K.A., Kromer, B., Manning, S.W., Muscheler, R., ... Talamo, S., 2020. The IntCal20 Northern Hemisphere radiocarbon age calibration curve (0–55 cal kBP). *Radiocarbon* 62(4), 725–757. <https://doi.org/10.1017/RDC.2020.41>
- Reitz, E.J., Wing, E.S., 2008. *Zooarchaeology* (second edition). Cambridge University Press, Cambridge, UK.
- Richter, J., 2016. Leave at the height of the party: a critical review of the Middle Paleolithic in Western Central Europe from its beginnings to its rapid decline. *Quatern. Int.* 411, 107–128. <https://doi.org/10.1016/j.quaint.2016.01.018>
- Roe, D.A., 1981. *The Lower and Middle Palaeolithic Periods in Britain*, 1st edition. Routledge, London. <https://doi.org/https://doi.org/10.4324/9781315747071>
- Ruebens, K., 2014. Late Middle Palaeolithic bifacial technologies across northwest Europe: typo-technological variability and trends. *Quatern. Int.* 350, 130–146. <https://doi.org/10.1016/j.quaint.2014.06.010>
- Ruebens, K., Smith, G.M., Fewlass, H., Sinet-Mathiot, V., Hublin, J.J., Welker, F., 2023. Neanderthal subsistence, taphonomy and chronology at Salzgitter-Lebenstedt (Germany): a multifaceted analysis of morphologically unidentifiable bone. *J. Quatern. Sci.* 38(4), 471–487. <https://doi.org/10.1002/jqs.3499>
- Schwartz-Narbonne, R., Longstaffe, F.J., Kardynal, K.J., Druckenmiller, P., Hobson, K.A., Jass, C.N., Metcalfe, J.Z., Zazula, G., 2019. Reframing the mammoth steppe: insights from analysis of isotopic niches. *Quatern. Sci. Rev.* 215, 1–21. <https://doi.org/10.1016/j.quascirev.2019.04.025>
- Scott, K., 1986. *British Bone Caves: A taphonomic study of Devensian faunal assemblages*. Apollo, University of Cambridge Repository, Cambridge, UK.
- Scott, K., 2018. The Large Vertebrates From Picken's Hole, Somerset. *Proc. Univ. Bristol Spelaeol. Soc.* 27(3), 267–313.
- Sinet-Mathiot, V., Rendu, W., Steele, T.E., Spasov, R., Madelaine, S., Renou, S., Soulier, M.C., Martisius, N.L., Aldeias, V., Endarova, E., Goldberg, P., McPherron, S.J.P., Rezek, Z., Sandgathe, D., Sirakov, N., Sirakova, S., Sorressi, M., Tsanova, T., Turq, A., Hublin, J.-J., Welker, F., Smith, G.M., 2023. Identifying the unidentified fauna enhances insights into hominin subsistence strategies during the Middle to Upper Palaeolithic transition. *Archaeol. Anthropol. Sci.* 15(9), 139. <https://doi.org/10.1007/s12520-023-01830-4>
- Sinet-Mathiot, V., Smith, G.M., Romandini, M., Wilcke, A., Peresani, M., Hublin, J.J., Welker, F., 2019. Combining ZooMS and zooarchaeology to study Late Pleistocene hominin behaviour at Fumane (Italy). *Sci. Rep.* 9(1), 1–13. <https://doi.org/10.1038/s41598-019-48706-z>
- Smith, G.M., Ruebens, K., Zavala, E.I., Sinet-Mathiot, V., Fewlass, H., Pederzani, S., Jaouen, K., Mylopotamitaki, D., Britton, K., Rougier, H., Stahlschmidt, M., Meyer, M., Meller, H., Dietl, H., Orschiedt, J., Krause, J., Schüler, T., McPherron, S.P., Weiss, M., Hublin, J.-J., Welker, F., 2024. The ecology, subsistence and diet of ~45,000-year-old *Homo sapiens* at Ilsehöhle in Ranis, Germany. *Nat. Ecol. Evol.* 8(3), 564–577. <https://doi.org/10.1038/s41559-023-02303-6>
- Stevens, R.E., Reade, H., Tripp, J., Sayle, K.L., Walker, E.A., 2021. Changing environment at the Late Upper Palaeolithic site of Lynx Cave, North Wales. In: Gaudzinski-Windheuser, S., Jöris, O. (Eds.), *The Beef Behind All Possible Pasts: The Tandem Festschrift in Honour of Elaine Turner and Martin Street, 157(Mainz)*. Römisch-Germanischen Zentralmuseums, Mainz, pp. 589–067. <https://doi.org/10.11588/propylaeum.950.c12581>
- Stiner, M.C., Kuhn, S.L., 2006. Changes in the “connectedness” and resilience of Paleolithic societies in Mediterranean ecosystems. *Hum. Ecol.* 34(5), 693–712. <https://doi.org/10.1007/s10745-006-9041-1>
- Strohm, M., Kavan, D., Novák, P., Volný, M., Havlíček, V., 2010. MMass 3: a cross-platform software environment for precise analysis of mass spectrometric data. *Anal. Chem.* 82(11), 4648–4651. <https://doi.org/10.1021/ac100818g>
- Sutcliffe, A.J., 1970. Spotted hyaena: crusher, gnawer, digester and collector of bones. *Nature* 227(5263), 1110–1113. <https://doi.org/10.1038/2271110a0>
- Sutcliffe, A.J., Zeuner, F.E., 1962. Excavations in the Torbryan Caves, Devonshire. 1. Tornewton Cave. *Proc. Devon*

- Archaeol. Explor. Soc. 5, 127–145.
- Tratman, E.K., 1964. Picken's Hole, Crook Peak, Somerset. A Pleistocene Site. Proc. Univ. Bristol Spelaeol. Soc. 10(2), 112–115.
- Tratman, E.K., Donovan, D.T., Campbell, J.B., 1971. The hyaena den (Wookey Hole), Mendip Hills, Somerset. Proc. Univ. Bristol Spelaeol. Soc. 12(3), 245–279.
- van Doorn, N.L., Hollund, H., Collins, M.J., 2011. A novel and non-destructive approach for ZooMS analysis: ammonium bicarbonate buffer extraction. Archaeol. Anthropol. Sci. 3(3), 281–289. <https://doi.org/10.1007/s12520-011-0067-y>
- Villa, P., Mahieu, E., 1991. Breakage patterns of human long bones. J. Hum. Evol. 21(1), 27–48. [https://doi.org/10.1016/0047-2484\(91\)90034-S](https://doi.org/10.1016/0047-2484(91)90034-S)
- Sinet-Mathiot, V., Rendu, W., Steele, T.E., Spasov, R., Madelaine, S., Renou, S., Soulier, M.-C., Martisius, N.L., Aldeias, V., Enderova, E., Goldberg, P., McPherron, S.J.P., Rezek, Z., Sandgathe, D., Sirakov, N., Sirakova, S., Soressi, M., Tsanova, T., Turq, A., Hublin, J.-J., Welker, F., Smith, G.M., 2023. Identifying the unidentified fauna enhances insights into hominin subsistence strategies during the Middle to Upper Palaeolithic transition. Archaeol. Anthropol. Sci. 15(9), 1–18. <https://doi.org/10.1007/s12520-023-01830-4>
- Wang, N., Brown, S., Ditchfield, P., Hebestreit, S., Koziłlikin, M., Luu, S., Wedage, O., Grimaldi, S., Chazan, M., Horwitz Kolska, L., Spriggs, M., Summerhayes, G., Shunkov, M., Richter Korzow, K., Douka, K., 2021. Testing the efficacy and comparability of ZooMS protocols on archaeological bone. J. Proteomics 233, 104078. <https://doi.org/10.1016/j.jprot.2020.104078>
- Watson, J.P.N., 1972. Fragmentation analysis of animal bone samples from archaeological sites. Archaeometry 14(2), 221–228. <https://doi.org/10.1111/j.1475-4754.1972.tb00064.x>
- Watson, J.P.N., 1979. The estimation of the relative frequencies of mammalian species: Khirokitia 1972. J. Archaeol. Sci. 6(2), 127–137. [https://doi.org/10.1016/0305-4403\(79\)90058-X](https://doi.org/10.1016/0305-4403(79)90058-X)
- Welker, F., Hajdinjak, M., Talamo, S., Jaouen, K., Dannemann, M., David, F., Julien, M., Meyer, M., Kelso, J., Barnes, I., Brace, S., Kamminga, P., Fischer, R., Kessler, B.M., Stewart, J.R., Pääbo, S., Collins, M.J., Hublin, J.-J., 2016. Palaeoproteomic evidence identifies archaic hominins associated with the Châtelperronian at the Grotte du Renne. Proc. Nat. Acad. Sci. U.S.A. 113, 11162–11167. <https://doi.org/10.1073/pnas.1605834113>
- Welker, F., Soressi, M., Rendu, W., Hublin, J.J., Collins, M., 2015. Using ZooMS to identify fragmentary bone from the Late Middle/Early Upper Palaeolithic sequence of Les Cottés, France. J. Archaeol. Sci. 54, 279–286. <https://doi.org/10.1016/j.jas.2014.12.010>
- White, M.J., Pettitt, P.B., 2011. The British late Middle Palaeolithic: an interpretative synthesis of Neanderthal occupation at the northwestern edge of the Pleistocene world. J. World Prehist. 24, 25–97. <https://doi.org/10.1007/s10963-011-9043-9>
- Wolverton, S., 2002. NISP: MNE and %whole in analysis of prehistoric carcass exploitation. N. Am. Archaeol. 23(2), 85–100. <https://doi.org/10.2190/EGDQ-CO1Q-LLD2-H3TP>
- Wragg Sykes, R.M., 2017. Neanderthals in the outermost west: technological adaptation in the late Middle Palaeolithic (re)-colonization of Britain, Marine Isotope Stage 4/3. Quatern. Int. 433, 4–32. <https://doi.org/10.1016/j.quaint.2015.12.087>
- Wragg Sykes, R.M., 2018. Picken's Hole, Crook Peak, Somerset: a description of the lithic collection and its probable late Middle Palaeolithic context. Proc. Univ. Bristol Spelaeol. Soc. 27(3), 315–338.

# Special Issue: Integrating ZooMS and Zooarchaeology: Methodological Challenges and Interpretive Potentials

## Supplement 1: Integrating Morphology and ZooMS-Identified Fauna Provides Insights Into Species Diversity and Neanderthal-Carnivores Interactions in Shared Landscapes: Evidence From Picken's Hole, Britain

FIONA HOLLORAN

*UCL Institute of Archaeology, 31-34 Gordon Square, London WC1H 0PY, UNITED KINGDOM; [fiona.holloran.19@ucl.ac.uk](mailto:fiona.holloran.19@ucl.ac.uk)*

DELPHINE FRÉMONDEAU

*UCL Institute of Archaeology, 31-34 Gordon Square, London WC1H 0PY, UNITED KINGDOM; [d.fremondeau@ucl.ac.uk](mailto:d.fremondeau@ucl.ac.uk)*

LINDA WILSON

*University of Bristol Spelaeological Society, Bristol, BS8 1TH UNITED KINGDOM; [lindawilson@coly.org.uk](mailto:lindawilson@coly.org.uk)*

LOUISE MARTIN

*UCL Institute of Archaeology, 31-34 Gordon Square, London WC1H 0PY, UNITED KINGDOM; [louise.martin@ucl.ac.uk](mailto:louise.martin@ucl.ac.uk)*

RHIANNON E. STEVENS

*UCL Institute of Archaeology, 31-34 Gordon Square, London WC1H 0PY, UNITED KINGDOM; [rhiannon.stevens@ucl.ac.uk](mailto:rhiannon.stevens@ucl.ac.uk)*

### SUPPLEMENT 1

This supplementary material includes: Supplementary Tables 1–13.

Supplement 2: R scripts and data for the figures, tables, and statistical tests: link(s) added to final proofs (<https://doi.org/10.5281/zenodo.13213101>).

Supplement 3: R scripts and MALDI output (.mzml) files used for processing ZooMS spectra (<https://doi.org/10.5281/zenodo.13940439>)

Catalogue No.	Context	Species	Specimen Type	Lab No.	<sup>14</sup> C Age BP	Error	95.4% Cal Age BP	
							From	To
M30.2/374	Unit 3	Woolly rhinoceros	Left femur	OxA-10804	40200	700	45835	39940
M30.2/159	Unit 3	Woolly rhinoceros	Mandibular symphysis	OxA-10805	>44000		Not calibrated	
M30.2/614	?*	Giant deer	Left cubonavicular	OxA-19091	>48200		Not calibrated	
M30.22/218	Unit 3?***	Horse	Tooth	OxA-19346	12460	60	Not calibrated	
M30.22/444	Unit 3B	Woolly rhinoceros	Tooth	OxA-22219	37200	800	43680	37115
M30.22/310	Unit 3B	Woolly rhinoceros	Tooth	OxA-22220	43000	1700	53055	39895
M30.22/19	Unit 3?***	Woolly rhinoceros	Tooth	OxA-22221	40300	1200	53055	38805
M30.22/187	Unit 3	Horse	Tooth	OxA-22222	45900	2400	53055	40605
M30.22/114	Unit 3	Horse	Tooth	OxA-22223	43100	1700	53055	39970
M30.22/1012	Unit 3	Woolly rhinoceros	Tooth	OxA-22277	40700	1300	53055	38925
M30.22/74	Unit 3A	Horse	Tooth	OxA-24997	46000	2400	53055	40645

*Table S1: Ultra-filtered uncalibrated radiocarbon dates (BP) and calibrated radiocarbon dates (cal BP) for faunal remains from Unit 3 at Picken's Hole. Lab numbers and uncalibrated radiocarbon ages are reported in Mullen 2018. \* Context not recorded in catalogue. \*\* Context disturbed by badger burrows. \*\*\*Reason for uncertainty not recorded in catalogue. Uncalibrated dates were retrieved from the ORAU database and IntCal20 was used for calibration using OxCal online (<https://c14.arch.ox.ac.uk/oxcal/OxCal.html> 30/01/2024).*

Size Category	Example Species	Estimated body weight (kg)
3: Medium-small	Grey wolf; arctic fox; spotted hyaena; reindeer; saiga	<100
5: Medium	Red deer; lion; elk, bear	100 – 400
7: Medium-large	Horse; aurochs; bison; giant deer	400 – 1000
9: Large	Woolly rhinoceros; woolly mammoth	>1500
0: Indeterminate	N/A	N/A

*Table S2: Mammal size classes used. Adapted from Bunn et al. (1986) and Marra (2013) with weight estimations from Meloro et al. 2007).*



ZoomS result	Species estimate	3B		3D		Total Unit 3	
		NISP	%NISP	NISP	%NISP	NISP	%NISP
<i>Canis lupus/Vulpes lapogus</i>	<i>Canis lupus/Vulpes lapogus</i>	0	0	2	0.33	2	0.3
<i>Vulpes vulpes</i>	<i>Vulpes vulpes</i>	0	0	3	0.5	3	0.4
Felidae/Monodontidae	<i>Crocuta crocuta/Panthera sp.</i>	8	7.62	44	7.3	52	7.7
<i>Rangifer tarandus</i>	<i>Rangifer tarandus</i>	20	19.05	145	24.05	165	24.3
Ursidae	<i>Ursus sp.</i>	0	0	5	0.83	5	0.7
<i>Cervid/Saiga</i>	<i>Cervus sp./Megaloceros sp.</i>	8	7.62	38	6.3	46	6.8
<i>Bos/Bison</i>	<i>Bos sp./Bison sp.</i>	5	4.76	33	5.47	38	5.6
Equidae	<i>Equus sp.</i>	10	9.52	73	12.11	83	12.2
Elephantidae	<i>Mammuthus primigenius</i>	5	4.76	37	6.14	42	6.2
Rhinocerotidae	<i>Coelodonta antiquitatis</i>	41	39.05	200	33.17	241	35.5
<i>Bos/Bison/Rangifer tarandus</i>		2	1.9	0	0	2	0.3
<b>Total identified samples</b>		<b>99</b>	<b>94.29</b>	<b>580</b>	<b>96.19</b>	<b>679</b>	<b>95.9</b>
<b>Total failed samples</b>		<b>6</b>	<b>5.71</b>	<b>23</b>	<b>3.81</b>	<b>29</b>	<b>4.1</b>
<b>Total analysed</b>		<b>105</b>	<b>100</b>	<b>603</b>	<b>100</b>	<b>708</b>	<b>100</b>

Table S3: ZooMS identification results from Picken's Hole, sub-contexts 3B and 3D within Unit 3.

ZooMS Identification	ZooMS-NISP	Max. Dim. (cm)	
		Median	IQR
<i>Rangifer tarandus</i>	165	3	1.8
<i>Crocuta crocuta/Panthera leo</i>	52	4	2.2
<i>Canis lupus/Vulpes lapogus</i>	2	3.3	0.1
<i>Vulpes vulpes</i>	3	2.1	0.5
<i>Cervus elaphus/Megaloceros giganteus</i>	46	4	3
<i>Ursus arctos</i>	5	3	1.1
<i>Equus ferus</i>	83	3.8	1.9
<i>Bison bison</i>	38	3.8	2.5
<i>Coelodonta antiquitatis</i>	241	3.5	2.1
<i>Mammuthus primigenius</i>	42	3.7	2
<b>Total</b>	<b>677</b>	<b>3.5</b>	<b>2.2</b>

Table S4: ZooMS number of identified specimens (NISP) from Picken's Hole, unit 3, according to taxon showing maximum dimension (cm) median and interquartile range (IQR).

	<i>Crocuta crocuta/Panthera leo</i>	<i>Rangifer tarandus</i>	<i>Cervus elaphus/Megaloceros giganteus</i>	<i>Bison bison</i>	<i>Equus ferus</i>	<i>Mammuthus primigenius</i>	<i>Coelodonta antiquitatis</i>
<i>Crocuta crocuta/Panthera leo</i>		<b>0.002</b>	0.336	0.65	0.343	0.827	0.303
<i>Rangifer tarandus</i>	0.283		<b>0.014</b>	<b>0.029</b>	<b>0.012</b>	<b>0.015</b>	<b>0.026</b>
<i>Cervus elaphus/Megaloceros giganteus</i>	0.175	0.248		0.512	0.455	0.511	0.638
<i>Bison bison</i>	0.141	0.244	0.164		0.361	0.48	0.116
<i>Equus ferus</i>	0.151	0.215	0.143	0.165		0.991	0.536
<i>Mammuthus primigenius</i>	0.116	0.255	0.157	0.165	0.065		0.763
<i>Coelodonta antiquitatis</i>	0.148	0.149	0.12	0.191	0.102	0.112	

Table S5: Kolmogrov-Smirnov test for similarity in the distribution of maximum dimensions (cm) of ZooMS identified taxon fragments (with no control for mammal size class) from Picken's Hole, Unit 3. Shaded cells are p-values, unshaded cells are the test statistic (maximum difference, D). Applied using `ks.test()` from the R 'stats' package (<https://search.r-project.org/R/refmans/stats/html/ks.test.html>). P-values considered significant (<0.05) are in bold.

Identification	Morph-NISP									ZooMS-NISP								
	Antler/Horn/Tusk	Dentition	Cranial	Thorax	Limb	Feet	LBF	Indet.	Total	Antler/Horn/Tusk	Dentition	Cranial	Thorax	Limb	Feet	LBF	Indet.	Total
<i>Canis lupus/Vulpes lapogus</i>	0	31	2	14	15	50	0	0	<b>112</b>	0	0	0	1	0	0	0	1	<b>2</b>
<i>Vulpes vulpes</i>	0	0	0	0	0	0	0	0	<b>0</b>	0	0	0	1	0	0	2	0	<b>3</b>
<i>Crocuta crocuta/Panthera leo</i>	0	210	1	3	12	11	0	0	<b>237</b>	0	0	1	21	0	0	14	16	<b>52</b>
<i>Rangifer tarandus</i>	17	59	2	5	19	82	0	0	<b>184</b>	5	0	0	17	0	2	89	52	<b>165</b>
<i>Ursus arctos</i>	0	3	0	0	0	0	0	0	<b>3</b>	0	0	0	3	0	0	1	1	<b>5</b>
<i>Cervus elaphus/Megaloceros giganteus</i>	0	36	2	0	1	13	0	0	<b>52</b>	0	0	0	4	0	0	14	28	<b>46</b>
<i>Bison bison</i>	3	32	0	0	1	12	0	0	<b>48</b>	0	0	0	4	0	0	13	21	<b>38</b>
<i>Equus ferus</i>	0	157	0	0	4	0	0	0	<b>161</b>	0	0	1	16	0	0	28	38	<b>83</b>
<i>Mammuthus primigenius</i>	3	27	0	0	0	0	0	0	<b>30</b>	0	0	0	11	0	0	4	27	<b>42</b>
<i>Coelodonta antiquitatis</i>	0	150	1	0	3	7	0	0	<b>161</b>	0	0	1	109	0	0	9	122	<b>241</b>
<b>Total</b>	<b>23</b>	<b>705</b>	<b>8</b>	<b>22</b>	<b>55</b>	<b>175</b>	<b>0</b>	<b>0</b>	<b>988</b>	<b>5</b>	<b>0</b>	<b>3</b>	<b>187</b>	<b>0</b>	<b>2</b>	<b>174</b>	<b>306</b>	<b>677</b>

Table S6: Comparison of body part representation according to morphological and ZooMS identified taxa from Pickens Hole, Unit 3.

ZooMS Identification	Light Weathering NISP	Adjusted residuals (light)	Moderate weathering NISP	Adjusted residuals (moderate)	Relatively heavy weathering NISP
<i>Crocota crocuta/Panthera leo</i>	21	0.3	19	<b>-2.91</b>	12
<i>Rangifer tarandus</i>	129	<b>8.81</b>	32	1.28	4
<i>Cervus elaphus/Megaloceros giganteus</i>	25	1.42	16	-0.57	5
<i>Bison bison</i>	18	0.51	15	-0.69	5
<i>Equus ferus</i>	41	0.56	36	0.83	6
<i>Mammuthus primigenius</i>	10	<b>-2.78</b>	26	0.05	6
<i>Coelodonta antiquitatis</i>	53	<b>-8.9</b>	157	1.26	31
Insufficient peptides	11	1.21	6	-0.43	2
No collagen	5	0.7	3	-1.2	2
<b>Composite X<sup>2</sup> Values</b>		<b>122</b>		<b>13</b>	

Table S7: Differences in number of identified specimens (NISP) across 'light' to 'relatively heavy' weathering stages (stages1 - 3: Behrensmeyer 1978) according to ZooMS identified taxon. Tested with composite chi-squared value and adjusted residuals, using `chisq_test()` and `shapiro.test()`, to confirm residuals are normally distributed, from the R 'rstatix' package (Carlson 2017; Grayson and Delpech 2003; Ruebens et al. 2023). Values over 1.96 (>95%) are considered significant and are in bold.



	Light	Moderate	Relatively Heavy
Light		0.1548	<b>0.0041</b>
Moderate	0.0898		<b>0.0004</b>
Relatively Heavy	0.2282	0.2699	

Table S8: Kolmogrov-Smirnov test for similarity in the distribution of maximum dimensions (cm) across observed weathering stages for all ZooMS samples (n=708) from Picken's Hole, Unit 3. Shaded cells are p-values, unshaded cells are the test statistic (maximum difference, D). Applied using `ks.test()` from the R 'stats' package (<https://search.r-project.org/R/refmans/stats/html/ks.test.html>). P-values considered significant (<0.05) are in bold.

ZooMS Identification	Break morphology	Burning	Butchery	Impact scar	Total NISP
<i>Rangifer tarandus</i>	Dry	3	0	2	4
	Mixed	2	3	6	9
<i>Crocuta crocuta/Panthera leo</i>	Dry	1	0	2	3
	Mixed	0	1	5	5
<i>Cervus elaphus/Megaloceros giganteus</i>	Dry	2	0	0	2
	Mixed	0	0	4	4
<i>Ursus arctos</i>	Mixed	0	0	2	2
<i>Equus ferus</i>	Dry	1	0	1	2
	Fresh	0	0	1	1
	Mixed	2	2	7	9
<i>Bison bison</i>	Dry	2	0	0	2
	Mixed	1	0	3	3
<i>Coelodonta antiquitatis</i>	Dry	8	1	5	12
	Fresh	0	0	2	2
	Mixed	2	0	17	18
<i>Mammuthus primigenius</i>	Dry	0	0	1	1
	Fresh	0	0	1	1
	Mixed	0	0	2	2
Unanalyzed	Dry	29	1	19	47
	Fresh	0	0	4	4
	Mixed	4	0	67	70
No collagen	Dry	1	0	0	1
<b>Total observations</b>		<b>58</b>	<b>8</b>	<b>151</b>	<b>204</b>

*Table S9: Summary of possible human bone surface modifications observed on ZooMS-identified and unanalyzed indeterminate bone fragments from Picken's Hole, Unit 3 (data from this study).*

ZooMS Identification	Absent	Adjusted residuals (absent)	Gnawing	Adjusted residuals (gnawing)	Digestion
<i>Crocuta crocuta/Panthera leo</i>	22	1.41	18	<b>3.9</b>	12
<i>Rangifer tarandus</i>	42	0.45	48	<b>2.87</b>	75
<i>Cervus elaphus/Megaloceros giganteus</i>	9	-0.92	16	<b>2.03</b>	21
<i>Bison bison</i>	9	0.03	11	1.13	18
<i>Equus ferus</i>	13	-0.49	19	-0.3	51
<i>Mammuthus primigenius</i>	8	-0.02	10	0.1	24
<i>Coelodonta antiquitatis</i>	20	-1.38	35	<b>-5.41</b>	186
Insufficient peptides	6	1.35	3	-0.45	10
No collagen	2	0.21	2	-0.23	6
<b>Composite X<sup>2</sup> Values</b>		<b>6.2</b>		<b>44</b>	

Table S10: Differences in number of identified specimens (NISP) across carnivore bone surface modification categories according to ZooMS identified taxon. Tested with composite chi-squared value and adjusted residuals, using `chisq_test()` and `shapiro.test()`, to confirm residuals are normally distributed, from the R 'rstatix' package (Carlson 2017; Grayson and Delpech 2003; Ruebens et al. 2023). 'AR' represents the adjusted residuals for the column to the left of it. Values over 1.96 (>95%) are considered significant and are in bold.

	Absent	Gnawing	Digestion
Absent		0.196	<b>3.6e-04</b>
Gnawing	0.125		<b>2.1e-07</b>
Digestion	0.206	0.2604	

Table S11: Kolmogrov-Smirnov test for similarity in the distribution of maximum dimensions (cm) across observed carnivore bone surface modification for all ZooMS samples (n=708) from Picken's Hole, Unit 3. Shaded cells are p-values, unshaded cells are the test statistic (maximum difference, D). Applied using `ks.test()` from the R 'stats' package (<https://search.r-project.org/R/refmans/stats/html/ks.test.html>). P-values considered significant (<0.05) are in bold.



ZooMS Identification	Absent	Gnawing	Digestion
<i>Crocuta crocuta/Panthera leo</i>	<b>Absent</b>	0.37	3.68e-01
	<b>Gnawing</b>	0.26	8.93e-02
	<b>Digestion</b>	0.3	0.44
<i>Rangifer tarandus</i>	<b>Absent</b>	0.58	<b>1.45e-05</b>
	<b>Gnawing</b>	0.15	<b>2.23e-06</b>
	<b>Digestion</b>	0.44	0.46
<i>Cervus elaphus/Megaloceros giganteus</i>	<b>Absent</b>	0.24	1.84e-01
	<b>Gnawing</b>	0.39	1.18e-01
	<b>Digestion</b>	0.41	0.37
<i>Bison bison</i>	<b>Absent</b>	0.39	6.99e-01
	<b>Gnawing</b>	0.36	5.15e-02
	<b>Digestion</b>	0.28	0.48
<i>Equus ferus</i>	<b>Absent</b>	0.73	1.02e-01
	<b>Gnawing</b>	0.22	<b>2.61e-02</b>
	<b>Digestion</b>	0.36	0.37
<i>Mammuthus primigenius</i>	<b>Absent</b>	0.69	1.29e-01
	<b>Gnawing</b>	0.3	2.78e-01
	<b>Digestion</b>	0.46	0.34
<i>Coelodonta antiquitatis</i>	<b>Absent</b>	0.62	5.00e-01
	<b>Gnawing</b>	0.19	<b>4.80e-03</b>
	<b>Digestion</b>	0.18	0.3

Table S12: Kolmogrov-Smirnov test for similarity in the distribution of maximum dimensions (cm) across observed weathering stages for each of the major taxa (n=667) identified using ZooMS from Picken's Hole, Unit 3. Shaded cells are p-values, unshaded cells are the test statistic (maximum difference, D). Applied using `ks.test()` from the R 'stats' package (<https://search.r-project.org/R/refmans/stats/html/ks.test.html>). P-values considered significant (<0.05) are in bold.

ZooMS Identification	Absent						Gnawing						Digestion					
	Antler/Horn/Tusk	Cranial	Thorax	Feet	LBF	Indet.	Antler/Horn/Tusk	Cranial	Thorax	Feet	LBF	Indet.	Antler/Horn/Tusk	Cranial	Thorax	Feet	LBF	Indet.
<i>Rangifer tarandus</i>	0	0	5	1	30	6	1	0	1	0	39	7	4	0	11	1	20	39
<i>Crocuta crocuta/Panthera leo</i>	0	1	9	0	6	6	0	0	7	0	5	6	0	0	5	0	3	4
<i>Canis lupus/Vulpes lapogus</i>	0	0	1	0	0	1	0	0	0	0	0	0	0	0	0	0	0	0
<i>Vulpes vulpes</i>	0	0	1	0	0	0	0	0	0	0	2	0	0	0	0	0	0	0
<i>Cervus elaphus/Megaloceros giganteus</i>	0	0	1	0	3	5	0	0	2	0	8	6	0	0	1	0	3	17
<i>Ursus arctos</i>	0	0	0	0	1	0	0	0	3	0	0	0	0	0	0	0	0	1
<i>Equus ferus</i>	0	0	2	0	5	6	0	1	4	0	6	8	0	0	10	0	17	24
<i>Bison bison</i>	0	0	1	0	3	5	0	0	1	0	8	2	0	0	2	0	2	14
<i>Coelodonta antiquitatis</i>	0	1	12	0	1	6	0	0	16	0	6	13	0	0	81	0	2	103
<i>Mammuthus primigenius</i>	0	0	2	0	0	6	0	0	4	0	2	4	0	0	5	0	2	17
<b>Total</b>	<b>0</b>	<b>2</b>	<b>34</b>	<b>1</b>	<b>49</b>	<b>41</b>	<b>1</b>	<b>1</b>	<b>38</b>	<b>0</b>	<b>76</b>	<b>46</b>	<b>4</b>	<b>0</b>	<b>115</b>	<b>1</b>	<b>49</b>	<b>219</b>

Table S13: Comparison of body part representation according to carnivore bone surface modifications for the ZooMS identified taxa from Pickens Hole, Unit 3.